Late Time Entropy Production in Leptogenesis Scenarios

Martin Nygård Breistein

Advisor: Jörn Kersten

A thesis presented for the degree of
Master of Science
December 20, 2016

UNIVERSITY OF BERGEN

Faculty of Mathematics and Natural Sciences
University of Bergen
Norway

Abstract

In this thesis we will consider Standard Model (SM) Leptogenesis scenarios and determine the maximally allowed entropy production with respect to the mass of the lightest right handed neutrino. We extend the SM Leptogenesis model as a Minimal Supersymmetric Standard Model (MSSM) to determine the viability of the Stau as the next to lightest supersymmetric particle (NLSP). We consider the viability of the Stau NLSP by taking into account the entropy dilution factor found in the MSSM Leptogenesis scenario and considering Big Bang Nucleosynthesis constraints.

Contents

Chapter 1

Introduction

Leptogenesis is an attractive model of baryogenesis for creating a lasting matter-antimatter asymmetry in the early universe. In the extended Standard Model the right handed neutrinos are very massive, between the order of $10^9 \sim 10^{15}$ GeV, and their CP-violating decays is the key to how Leptogenesis can generate such an matter-antimatter asymmetry. Leptogenesis also requires the mass of the left handed neutrinos to be less than 0.1 eV, and because of the see-saw mechanism, we find Leptogenesis to be consistent with this range of masses for the right handed neutrinos. In the process of Leptogenesis, these right handed neutrinos decay out of thermal equilibrium into either a set of a lepton and a Higgs, lH, or an anti-lepton and an anti-Higgs $\bar{l}\bar{H}$. These decays, and the interactions between the decay products, are represented with a set of Boltzmann equations (included in chapter 3.4), which determines the maximal Baryon-Lepton asymmetry available.

In this thesis we extend the simplest model of leptogenesis into MSSM and explore the possibility of the Stau as the Next lightest supersymmetric particle. By extending the model into MSSM, we further complicate the model as we have to introduce the sneutrino, the super symmetric partner of the neutrino, as an additional decaying particle, and introduce new decay channels for the neutrino. As a constraint on the Stau abundance, we consider how massive, long lived, charged particles will effect the abundances generated from Big Bang Nucleosynthesis.

In Chapter 1 we will explore the mathematical framework of SM and MSSM, in addition to the see-saw mechanism and sphaleron processes both central to the mechanism of Leptogenesis. In Chapter 2 we expand on the cosmological underpinnings of the model of baryogenesis and outline the potential for entropy production in the early universe. Chapter 3 contains the calculations which determine the peak entropy production allowed in SM Leptogenesis, and the extension of the model into MSSM. Finally in Chapter 4 we utilize the peak entropy production available in the MSSM Leptogenesis scenario to calculate the Relic density of the Stau, in order to determine the viability of it as the Next to Lightest Supersymmetric Particle (NLSP) candidate.

Chapter 2

Particle Theory

2.1 The standard model

The standard model of particle physics is a mathematical framework which describes interactions between particles through three fundamental forces, which are the strong, weak and electromagnetic interactions. The motivation for this model of interactions is to unify these forces and introduce a mass generating mechanism for the fundamental particles, i.e. the Higgs mechanism. The structure of the standard model is fundamentally based upon quantum field theory, a model in which a lagrangian constructed from quantized fields determines the dynamics of particle interactions[1, 2].

Quantum Chromodynamics is a non-abelian gauge theory generated by symmetry group SU(3) which describes the strong interactions between quarks. The gauge bosons associated with the group $\mathrm{SU}_c(3)$ are the 8 spin one particles called gluons, G_i^μ. Any particles interacting with gluons, i.e. transforms under rotation of this group, are said to carry colour. These interactions are generally categorized as the strong interactions. The lagrangian determines the kinematics and dynamics of this model for massless quarks.

$$\begin{aligned} \mathcal{L}_{QCD} &= \bar{\psi}_q(i\not{D})\psi_q - \frac{1}{4}G_{i\mu\nu}G_i^{\mu\nu} \\ \not{D} &= \gamma^\mu D_\mu = \gamma^\mu(\partial_\mu + ig_s\frac{\lambda_i}{2}A_{\mu i}) \\ G_i^{\mu\nu} &= \partial^\mu A_i^\nu - \partial^\nu A_i^\mu + g_s f_{ijk}A_j^\mu A_k^\nu \end{aligned} \tag{2.1.1}$$

	l_R	l_L	ν_L
$\frac{Q}{e}$	-1	-1	0
I_3^W	0	$-1/2$	$+1/2$
Y	-1	$-1/2$	$-1/2$

Table 2.1.1: Hypercharge for right handed and left handed leptons.

Electro-weak theory, constructed from unifying Quantum electrodynamics and weak-theory, is a non-abelian gauge theory generated from the symmetry group $\mathrm{SU}_L(2)\otimes\mathrm{U}_Y(1)$. There are 3 spin one bosons associated with $\mathrm{SU}_L(2)$, W_i^μ, where the L indicates that only left handed fermions are affected by this symmetry. There is only one spin one gauge boson associated with the $\mathrm{U}_Y(1)$ symmetry, B_μ, where the Y denotes the weak hypercharge. The combined 4 spin one particles which describe $\mathrm{SU}_L(2)\otimes\mathrm{U}_Y(1)$ are different from the gluons mentioned above as the interaction state and mass state are not congruent. Consequently the physical bosons which mediate the weak interaction, $\mathrm{W}^\pm$, Z^0 and the photon, arise as a result of mixing between the gauge bosons. This manifests itself in the weak mixing angle, which is important in determining the masses of these particles. The particle chirality becomes extremely relevant for this interaction as well, as the right handed leptons do not interact with the massive $W^\pm$ bosons, and additionally there are no right handed neutrinos as these right handed leptons also do not have any $SU(2)$ gauge interactions. Moreover the hypercharge, defined as $Y = \frac{Q}{e} - \mathcal{I}_3^W$, for the right handed leptons is different from the left handed as they do not take part in the neutral current $\mathcal{I}_3^W$. The Lagrangian for massless leptons is given as:

$$\begin{aligned}\mathcal{L}_{EW} = \bar{\Psi}_l^L(i\not{D}_L)\Psi_l^L + \bar{\psi}_l^R(i\not{D}_R)\psi_l^R - \frac{1}{4}W^i_{\mu\nu}W_i^{\mu\nu} - \frac{1}{4}B_{\mu\nu}B^{\mu\nu} \\ D_{\mu L} = \partial_\mu + ig\frac{\tau_i}{2}W_i^\mu - ig'\frac{1}{2}B_\mu \\ D_{\mu R} = \partial_\mu - ig'B_\mu\end{aligned} \tag{2.1.2}$$

In the standard model there are 12 spin one gauge bosons which follows from the its gauge group $\mathrm{SU}_c(3)\otimes\mathrm{SU}_L(2)\otimes\mathrm{U}_Y(1)$ and the additional scalar boson (the Higgs boson) which arises from the Higgs mechanism. This Higgs mechanism is

also responsible for generating the mass of the fermions, the $W^{\pm}$ and Z bosons.

$$\mathcal{L}_{SM} = \mathcal{L}_{quarks} + \mathcal{L}_{leptons} + \mathcal{L}_{gluons} + \mathcal{L}_{W,B} + \mathcal{L}_{Higgs} + \mathcal{L}_{qH} + \mathcal{L}_{lH} \quad (2.1.3)$$

The SM lagrangian includes the interaction and kinematic terms for both strong and electro-weak interactions, $\mathcal{L}_{quarks} + \mathcal{L}_{leptons} + \mathcal{L}_{gluons} + \mathcal{L}_{W,B}$, the Higgs self interaction and mass term, $\mathcal{L}_{Higgs}$, as well as the mass generating terms for the leptons and quarks ,$\mathcal{L}_{qH} + \mathcal{L}_{lH}$. Within this model there are 6 leptons $e, \mu, \tau, \nu_e, \nu_\mu, \nu_\tau$, defined as particles which do not interact strongly, and 6 hadrons u, d, c, s, t, b defined as particles which do interact strongly.

The Higgs mechanism explains how fundamental particles such as quarks and the charged leptons gain mass through electro-weak symmetry breaking. Both $\mathcal{L}_{lH} + \mathcal{L}_{qH}$ are of the form $\bar{\psi'}^L \boldsymbol{Y} \phi \psi'^R$, where Y is the Yukawa coupling and H denotes the Higgs field, $\phi = \frac{1}{\sqrt{2}}(V + H, 0)^T$. For the leptons the Yukawa coupling is a 3x3 diagonalized matrix, but for the quark sector the story is more complicated. Since the Yukawa interactions from down type quarks $\bar{\psi'}^L_q \boldsymbol{Y} \phi \psi'^R_{d_q}$ conserves hypercharge it is gauge invariant, but as the Yukawa interaction for uptype quarks $\bar{\psi'}^L_q \boldsymbol{Y} \phi \psi'^R_{u_q}$ does not conserve hypercharge they are not permitted. Therefore we introduce the charge conjugate of the Higgs field to remedy this, $\tilde{\phi} = i\tau_2 \phi = \frac{1}{\sqrt{2}}(0, V + H)^T$[1].

$$\begin{aligned} \mathcal{L}_{qH} &= -\bar{\Psi'}^L_p \boldsymbol{Y}_{pq} \phi \psi'^R_{u_q} - \bar{\Psi'}^L_p \boldsymbol{Y}_{pq} \tilde{\phi} \psi'^R_{d_q} + h.c. \\ &= -\bar{\Psi'}^L_p M^u_{pq} \psi'^R_{u_q} - \bar{\Psi'}^L_p M^d_{pq} \psi'^R_{d_q} \\ &- \bar{\Psi'}^L_p \frac{M^u_{pq}}{V} \psi'^R_{u_q} H - \bar{\Psi'}^L_p \frac{M^d_{pq}}{V} \psi'^R_{d_q} H + h.c. \end{aligned} \quad (2.1.4)$$

Where $\mathrm{M}^{u,d} = \frac{Y^{u,d} V}{\sqrt{2}}$ is the mass matrix which determines the mass for up type and down type quarks. These matrices are not diagonalized so we introduce a unitary transformation matrix $U^{L\dagger}_{\psi} M_{\psi} U^R_{\psi} = M_{diag}$, which transforms the gauge eigenstate into the mass eigenstate$\psi'^{L,R} = U^{L,R}_{\psi} \psi^{L,R}$. As it turns out this introduction of the unitary matrix has some interesting consequences when it comes to the charged current weak interaction, which only affect the left handed particles.

$$\begin{aligned} \mathcal{L}_{cc} &= \frac{-g}{\sqrt{2}} \left(\bar{u}^L U^L_u \gamma^\nu W_\nu U^L_D d'^L + h.c. \right) \\ &= \frac{-g}{\sqrt{2}} \left(\bar{u}^L V \gamma^\nu W_\nu d'^L + h.c. \right) \end{aligned} \quad (2.1.5)$$

Here, $V \equiv {U_u^L}^\dagger U_d^L$ is known as the "Cabibbo-Kobayashi-Maskawa" matrix which determines the mixing between the top type quarks.

2.2 MSSM

The Minimal Supersymmetric Standard Model is the simplest supersymmetric extension of the standard model, and is constructed by replacing every standard model field with a supermultiplet. Since the supersymmetry transforms a fermion into a boson or a boson into a fermion [3]

$$\begin{aligned} Q\,|Fermion\rangle &= |Boson\rangle \\ Q\,|Boson\rangle &= |Fermion\rangle \end{aligned} \tag{2.2.1}$$

the supermultiplet collects the pairs which transform into each other. Then for every scalar and spinor field we will introduce a chiral superfield, and for every vector field similarly a vector superfield.

$$(\nu_{L_i}) \to (\nu_{L_i}, \tilde{\nu}_{L_i}) \tag{2.2.2}$$

This doubles the number of existing particles in the standard model, while keeping the existing interactions between the SM particles unchanged. Another strength of this approach is that the superpartners of the SM particles all transform equivalently under gauge transformations G_{SM}. The Higgs sector introduces a second Higgs, as we cannot charge conjugate the Higgs field to generate mass for the down type quarks and the charged leptons as mentioned in the previous section. As such the SM Higgs potential is transformed from $\phi \to \phi_u$ and $\tilde{\phi} \to \phi_d$. When we construct the supersymmetric lagrangian, we will consider the gauge symmetries and the superpotential as the set of interactions allowed by the model. The gauge groups are maintained from SM and the super potential is of the form[3]

$$W_{MSSM} = \hat{U} Y^u \hat{Q} \hat{H}_u - \hat{D} Y^d \hat{Q} \hat{H}_d - \hat{E} Y^e \hat{L} \hat{H}_d + \mu \hat{H}_d \hat{H}_u \tag{2.2.3}$$

The lagrangian density for a fully normalizable supersymmetric theory is then determined by $\mathcal{L}_{gauge}$ and $\mathcal{L}_{chiral}$. The gauge transformations for vector superfields are:

$$\begin{aligned} A_\mu^a &\to A_\mu^a + \partial_\mu \Lambda^a + g f^{abc} A_\mu^b \Lambda^c \\ \lambda^a &\to \lambda^a + g f^{abc} \lambda^b \Lambda^c \end{aligned} \tag{2.2.4}$$

Particles	Superfields	spin 0	spin 1/2	SU(3)⊗SU(2)⊗U(1)
squarks, quarks	$\hat{Q}$	$(\tilde{u}_L, \tilde{d_L})$	(u_L, d_L)	$(\mathbf{3}, \mathbf{2}, \frac{1}{6})$
u= u, c, t	$\hat{U}$	$\tilde{u}_R^*$	$u_R^\dagger$	$(\bar{\mathbf{3}}, \mathbf{2}, -\frac{2}{3})$
d= d, s, b	$\hat{D}$	$\tilde{d}_R^*$	$d_R^\dagger$	$(\bar{\mathbf{3}}, \mathbf{2}, \frac{1}{3})$
sleptons, leptons	$\hat{L}$	$(\tilde{\nu}, \tilde{\ell}_L)$	(ν, ℓ_L)	$(\mathbf{1}, \mathbf{2}, -\frac{1}{2})$
$\ell = e, \mu, \tau$; $\nu = \nu_e, \nu_\mu, \nu_\tau$	$\hat{E}$	$\tilde{\ell}_R^*$	$\ell_R^\dagger$	$(\mathbf{1}, \mathbf{1}, 1)$
Higgs, higgsinos	$\hat{H}_u$	$(\mathcal{H}_u^+, \mathcal{H}_u^0)$	$(\tilde{\mathcal{H}}_u^+, \tilde{\mathcal{H}}_u^0)$	$(\mathbf{1}, \mathbf{2}, \frac{1}{2})$
	$\hat{H}_d$	$(\mathcal{H}_d^0, \mathcal{H}_d^-)$	$(\tilde{\mathcal{H}}_d^0, \tilde{\mathcal{H}}_d^-)$	$(\mathbf{1}, \mathbf{2}, -\frac{1}{2})$

Table 2.2.1: The chiral supermultiplets in MSSM and their gauge group representation.

Particles	Superfields	spin 1/2	spin 1	SU(3)⊗SU(2)⊗U(1)
gluino, gluon	$\hat{G}^a$	$\tilde{g}$	g	$(\mathbf{8}, \mathbf{1}, 0)$
wino, W bosons	$\hat{W}^i$	$\tilde{W}^\pm, \tilde{W}^0$	$(W^\pm, W^0)$	$(\mathbf{1}, \mathbf{3}, 0)$
bino, B bosons	$\hat{B}$	$\tilde{B}^0$	B^0	$(\mathbf{1}, \mathbf{1}, 0)$

Table 2.2.2: The gauge supermultiplets in MSSM and their gauge group representation.

Where A_μ is a massless gauge boson field, f^{abc} is the totally antisymmetric structure that defines the gauge group and λ^a is a two component Weyl fermion gaugino. The on-shell degrees of freedom associated with the two fields amounts to 2 fermionic helicity and 2 bosonic states. But for the off-shell degrees of freedom, the weyl fermion has 2 complex degrees of freedom (4 real degrees) where as the gauge boson only has 3 degrees; as such we introduce a real bosonic auxiliary field D^a so the theory becomes consistent off-shell. D^a can be expressed fully in terms of scalar fields, $D^a = -g(\phi^* T^a \phi)$, where T^a is the gauge group generator. This auxiliary field does not have any kinematic terms, is of dimension [mass]^2 and can be eliminated from the on-shell calculations by considering the trivial solution to the equation of motion $D^a = 0$. The lagrangian density for each gauge group is then also determined by a, which runs from 1-8 for $SU(3)_c$, 1-3 for $SU(2)_L$ and 1 for $U(1)_Y$.

$$\begin{aligned} \mathcal{L}_{gauge} =& -\frac{1}{4} F^a_{\mu\nu} F^{\mu\nu a} + i\lambda^{\dagger a} \bar{\sigma}^\mu \nabla_\mu \lambda^a + \frac{1}{2} D^a D^a \\ F^a_{\mu\nu} =& \partial_\mu A^a_\nu - \partial_\nu A^a_\mu + g f^{abc} A^b_\mu A^c_\nu \end{aligned} \tag{2.2.5}$$

The Chiral superfield's free particle lagrangian takes is of the form:

$$\mathcal{L}_{free} = -\partial^\mu \phi^{*i} \partial_\mu \phi + i\psi^{\dagger i} \bar{\sigma}^\mu \partial_\mu \psi_i + F^{*i} F_i \tag{2.2.6}$$

Where F_i is an auxiliary field, ϕ is a complex scalar field and ψ is a lefthanded Weyl fermion field. The transformation of these chiral fields which keep the free lagrangian invariant are

$$\begin{aligned} \phi_i &\to \phi_i + \epsilon\psi_i \\ (\psi_i)_\alpha &\to (\psi_i)_\alpha - i(\sigma^\mu \epsilon^\dagger)_\alpha \partial_\mu \phi_i + \epsilon_\alpha F_i \\ F_i &\to F_i - i\epsilon^\dagger \bar{\sigma}^\mu \partial_\mu \psi_i \end{aligned} \tag{2.2.7}$$

The interaction lagrangian is then determined by the interaction between the fields.

$$\mathcal{L}_{int} = -\frac{1}{2} W^{ij} \psi_i \psi_j + W^i F_i + c.c \tag{2.2.8}$$

The most general non-gauge interactions of chiral multiplets are determined by the superpotential, as both W^i and W^{ij} are defined as derivative of the super potential with respect to the scalar fields.

$$\begin{aligned} W^{ij} &= \frac{\delta^2}{\delta\phi_i \delta\phi_j} W \\ W^i &= \frac{\delta W}{\delta \phi_i} \end{aligned} \tag{2.2.9}$$

The combination of $\mathcal{L}_{free} + \mathcal{L}_{int}$ contains additional auxiliary field terms which determines the equations of motion $F^{*i} = -W^i$ and $F_i = -W^*{}_i$, and can therefore be expressed algebraically in terms of the scalar fields. We can chose to express $W_i W^i$ as a scalar potential, $V(\phi, \phi^*)$, given in terms of the super potential to further simplify the lagrangian. As such the total lagrangian for the chiral fields becomes[3]:

$$\mathcal{L}_{chiral} = -\partial^\mu \phi^{i*} \partial_\mu \phi + i\psi^{\dagger i} \bar{\sigma}^\mu \partial_\mu \psi_i - \frac{1}{2}(W^{ij} \psi_i \psi_j + W^{ij*} \psi_i^\dagger \psi_j^\dagger) - V(\phi, \phi^*) \tag{2.2.10}$$

By combining the chiral and gauge lagrangian supplemented by mixed terms which are unaffected by gauge transformations of the gauge and chiral fields, we obtain the MSSM lagrangian.

$$\mathcal{L} = \mathcal{L}_{chiral} + \mathcal{L}_{gauge} - \sqrt{2} g(\phi^* T^a \psi)\lambda^a - \sqrt{2} g \lambda^{a\dagger}(\psi^\dagger T^a \phi) + g(\phi^* T^a \phi) D^a \tag{2.2.11}$$

R-parity is a property that all MSSM interactions have to fulfil. All interactions must conserve R-parity, where we assign the value -1 to supersymmetric partners, and the value 1 to SM particles. Thus in an interaction which includes one supersymmetric particle in the initial state, the R-parity demands that there is an odd number of supersymmetric partners in the final state. As an example a process includes one initial SM particle and one initial supersymmetric partner $1 \times (-1) = (-1)$, the final state of the interaction must also conserve this property. Therefore in a two body final state for this interaction one of the final state particles has to be a SM particle and the other a supersymmetric partner.

2.3 See-saw Mechanism

The See-saw Mechanism is in principle a mathematical technique to explain why we can detect neutrino flavour oscillations for the left handed neutrinos, and why there exists a mass difference between the neutrinos and more massive standard model particles eg. quarks or leptons. The simplest extension of the standard model using this mechanism introduces three new massive right handed neutrino fields, which are unaffected by electroweak interactions[4]. The majorana mass term in the extended standard model lagrangian for the right handed neutrinos has the form:

$$\mathcal{L}^{\nu R}_{majorana} = -\frac{1}{2}\bar{\psi}_N M_R \psi_N \tag{2.3.1}$$

Where the Ψ_N is a mixed state of right handed neutrinos and the charged conjugated right handed neutrino field, which can be shown to be a left handed field.

$$\psi_N = \psi^R_\nu + \psi^{RC}_\nu \tag{2.3.2}$$

In addition to this mass term you can introduce the dirac mass term.

$$\mathcal{L}^{\nu}_{dirac} = -\bar{\psi}^R_\nu \frac{Y^\nu v}{\sqrt{2}} \psi^L_\nu \tag{2.3.3}$$

Now if we combine these terms into a lagrangian for the full neutrino mass terms, we see that we construct a mass-matrix of the form:

$$\mathcal{L}^{\nu}_{m} = -(\bar{\psi}^L_\nu, \bar{\psi}_N) \begin{pmatrix} 0 & M_D \\ M_D & M_R \end{pmatrix} (\psi^L_\nu, \psi_N) \tag{2.3.4}$$

To find the mass eigenstates we diagonalize this matrix.

$$\begin{aligned} \lambda(M_R - \lambda) - M_D^2 &= 0 \\ \lambda^2 - M_R\lambda - M_D^2 &= 0 \end{aligned} \tag{2.3.5}$$

Since the Majornana mass of the right handed neutrinos are significantly larger than the Dirac mass, we can use the limit $M_R \gg M_D$ find the mass eigenstates of the left handed neutrinos λ_- and right handed λ_+:

$$\begin{aligned} \lambda_+ &\approx M_R \\ \lambda_- &= \frac{M_R - \sqrt{M_R^2 + 4M_D^2}}{2} \end{aligned} \tag{2.3.6}$$

By expanding the square root we gain:

$$\frac{M_R}{2}\left(1 - \sqrt{1 + \frac{4M_D^2}{M_R^2}}\right) = \frac{M_R}{2}\left(1 - 1 - 2\frac{M_D^2}{M_R^2}\right) = -\frac{M_D^2}{M_R} \tag{2.3.7}$$

By varying the value of M_R we can effectively reduce the mass eigenstate of the left handed neutrino as low as we want, hence the name: The *see-saw* mechanism. We can now re-express this mass eigenstate as:

$$m_\nu = -m_D \frac{1}{M_R} m_D^T \tag{2.3.8}$$

2.4 Stau mixing

Stau mixing follows directly from the associated high mass of the stau[5]. It is the only slepton with a significant mixing between the right handed and left handed states. Unlike the SM analogue-fermions present in MSSM whose masses are generated from the superpotential Yukawa interaction, the Slepton's mass is generated from 4 distinct mass terms: Superpotential terms, soft SUSY breaking scalar mass, soft SUSY breaking trilinear terms and D-mass terms. The soft SUSY breaking trilinear terms are dependent on mixing terms between the left and right handed states. The D-mass and soft SUSY breaking scalar mass terms on the other hand contribute to the mass individually from both their left and right states. The superpotential contains both mixing terms between the left and right states. By collecting these terms, we can construct a mass matrix containing all 4 of these contributions to the stau mass.

$$\mathcal{L} \ni (\tilde{\tau}_L^\dagger, \tilde{\tau}_L^\dagger)\mathcal{M}_{\tilde{\tau}}^2(\tilde{\tau}_L, \tilde{\tau}_L)^T \tag{2.4.1}$$

Where $\mathcal{M}^2_{\tilde{\tau}}$ is constructed by the terms mentioned above:

$$\mathcal{M}^2_{\tilde{\tau}} \simeq \begin{pmatrix} m^2_{\tilde{\tau}_L} + m^2_\tau + D(\tilde{\tau}_L) & m_\tau(-A_\tau + \mu \cot\beta) \\ m_l(-A_\tau + \mu \cot\beta) & m^2_{\tilde{\tau}_R} + m^2_\tau + D(\tilde{\tau}_R) \end{pmatrix} \tag{2.4.2}$$

in which $m^2_{\tilde{\tau}_L}$ and $m^2_{\tilde{\tau}_R}$ are results of the soft SUSY breaking scalar masses, which are present regardless of whether or not electroweak symmetry is spontaneously broken.

The SUSY breaking trilinear terms are of the form $\mathcal{L} \ni -(-A_\tau m_\tau)(\tilde{\tau}^\dagger_L \tilde{\tau}_R + \tilde{\tau}_R \tilde{\tau}^\dagger_L)$ generated from the terms in the lagrangian for the soft SUSY breaking interaction between the slepton and Higgs bosons. These terms are not present if electroweak symmetry is unbroken; similarly the terms terms involving $\tilde{\tau}^\dagger_L \tilde{\tau}_R + h.c.$ generated from the super potential also disappear if EW-symmetry is unbroken. As a result, the off diagonal terms are absent if electroweak symmetry is not spontaneously broken. The D-terms are of the form:

$$\begin{aligned} D(\tilde{\tau}_L) =& M^2_Z \cos(2\beta)(-\frac{1}{2} + sin^2\theta_W) \\ D(\tilde{\tau}_L) =& M^2_Z \cos(2\beta)(-sin^2\theta_W) \end{aligned} \tag{2.4.3}$$

We now diagonalize the matrix to produce 2 mass states $\tilde{\tau}_{1,2}$ the in which $\tilde{\tau}_1$ is defined as the lighter of the two.

$$\begin{pmatrix} \tilde{\tau}_1 \\ \tilde{\tau}_2 \end{pmatrix} = \begin{pmatrix} \cos\theta_{\tilde{\tau}} & -\sin\theta_{\tilde{\tau}} \\ \sin\theta_{\tilde{\tau}} & \cos\theta_{\tilde{\tau}} \end{pmatrix} \begin{pmatrix} \tilde{\tau}_L \\ \tilde{\tau}_R \end{pmatrix} \tag{2.4.4}$$

By substituting in for the D-terms in eq. 2.4.2 before we diagonalize, we can obtain an expression for $\theta_{\tilde{\tau}}$ which determines the size of the mixing between the left handed and right handed stau.

$$\theta_{\tilde{\tau}} = \tan^{-1}\left(\frac{m^2_{\tilde{\tau}_L} + m^2_\tau + M^2_Z \cos(2\beta)(-\frac{1}{2} + sin^2\theta_W) - m^2_{\tau_1}}{m_\tau(-A_\tau + \mu \tan\beta} \right) \tag{2.4.5}$$

2.5 Sphaleron processes

The standard model of particle physics is extremely reliable way of determining electroweak (QFD) and strong (QCD) interactions through perturbation theory. But additionally there are processes allowed, or rather not prohibited, by the SM Lagrangian which violate many of the quantities conserved under interactions arising from perturbative methods. The sphaleron is one such process, as it is the classical set of solutions which minimizes the action and is therefore a minimum of the Lagrangian, similar to a saddle point in that it is an inherently unstable. Additionally since these processes do not conserve baryon and lepton number, because they are not derived from perturbation theory, and therefore they provide a unique mechanism for generating such a Baryon-lepton asymmetry in the early universe. For temperatures in the range $10^{12}\text{GeV} \gtrsim T \gtrsim 100\text{GeV}$ sphaleron processes are in equilibrium[6]. This temperature regime lines up well with the expected temperature expected from Leptogenesis. An example of one such process would be three baryons interact to produce 3 anti-leptons, or one quark into anti 2 quarks and one anti lepton.

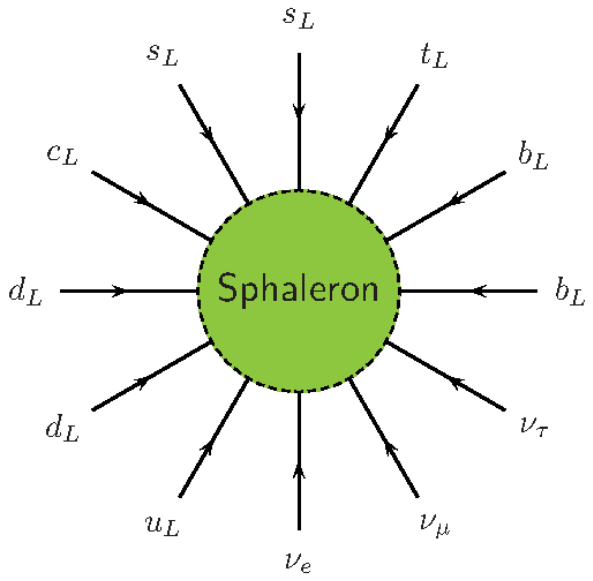

Figure 2.5.1: One of the 12 possible baryon+lepton violating sphaleron processes. Figure taken from [6]

Chapter 3

Cosmology

3.1 Entropy production

Entropy production in the early universe is fuelled by massive particles decaying out of equilibrium, as there can be no net gain in entropy for a system in equilibrium. This necessarily requires the particle to have decoupled from the heat bath and maintain an abundance larger than that of the equilibrium abundance, $Y \gg Y_{EQ}$. Take a particle species ψ, a long lived and non relativistic particle which has decoupled from the heat bath and has a pre-decay abundance of $\frac{n_\psi}{s}$. The particle species' energy density is proportional to R^{-3}, but since the radiation density is proportional to R^{-4}, it grows relative to it by a factor of R. Given the long lived nature of this particle species it will come to dominate the energy density of the universe. As such when it decays, it will generate a significant amount of entropy. When the particle decays at time $t \sim \tau$ since decoupling (where τ is mean lifetime of the particle), at temperature $T = T_D$ and the energy density of the universe, $\rho \sim \rho_\psi = sY_\psi m_\psi$. Before the decay, the temperature T_D and lifetime of the particle is related by[7]:

$$H^2(T_D) \equiv H_D^2 \sim G\rho \sim Y_\psi T_D^3 \frac{m_\psi}{m_{Pl}^2} \sim \tau^-2 \tag{3.1.1}$$

from which we can derive an expression for the temperature before decay:

$$T_D \sim \sqrt[3]{\frac{m_{Pl}^2}{Y_\psi m_\psi \tau^2}} \tag{3.1.2}$$

Based on the assumption that the particle will decay into relativistic particles which will rapidly thermalize, i.e. fall into thermal equilibrium. Assuming the decays happen instantaneous, this decay then yields ρ_R the radiation density of the universe after the decay of this massive particle.

$$\rho_R \sim g_* T_{RH}^4 \tag{3.1.3}$$

Because of energy conservation the energy density per comoving volume before, $H_D^2 m_{Pl}^2$, and after this decay we can express T_{RH} as:

$$T_{RH} \sim \sqrt[4]{\frac{H_D^2 m_{Pl}^2}{g_*}} \sim \sqrt[4]{\frac{m_{Pl}^2}{g_* \tau^2}} \tag{3.1.4}$$

Now the ratio between the entropy before and the entropy after the decay is expressed as

$$\frac{S_{after}}{S_{before}} = \frac{g_* R^3 T_{RH}^3}{g_* R^3 T_D^3} \sim \sqrt[4]{g_* \frac{Y_\psi^4 m_\psi^4 \tau^2}{m_{Pl}^2}} \tag{3.1.5}$$

In which S is the total entropy of the Universe. As a result of this, it appears the Universe is reheated from the particle species decay.

$$\frac{T_{after}}{T_{before}} = \frac{T_{RH}}{T_D} = \sqrt[3]{\frac{S_{after}}{S_{before}}} \tag{3.1.6}$$

Counter intuitively, in fact the temperature never increases, it only serves to slow the temperature decrease which would be realized in the absence of ψ. From this we can also find the relationship between the relative abundance Y_χ of other particles, before and after the decay, since the increase in entropy will affect the relative abundance as $Y_\chi = \frac{N_\chi}{s}$[8].

$$Y_\chi^{after} = \frac{1}{\Delta} Y_\chi^{before} \tag{3.1.7}$$

where $\Delta = \frac{S_{after}}{S_{before}}$ is the entropic dilution factor. For standard cosmology, where there is no entropy production, $\Delta = 1$. For alternative models such as Leptogenesis instances of entropy production may be required, and Δ may be take values larger than one in these cases, $\Delta \geq 1$.

3.2 Big Bang Nucleosynthesis

The model Big Bang Nucleosynthesis explains the mechanics of how the lighter elements (other than ^{1}H) are produced after e^+e^- annihilation epoch. Of special

importance is the temperature at the end of baryogenesis since it determines the amount of particles which are able to overcome the coulomb potential and bind into heavier elements. Consider a Nuclear statistical equilibrium[7],

$$n_A = g_A \left(\frac{m_A T}{2\pi}\right)^{\frac{3}{2}} \exp\left(\frac{\mu_A - m_A}{T}\right) \tag{3.2.1}$$

where a non-relativistic particle species A(Z), with mass number A and charge Z, has the chemical potential μ_A. This equation also holds for both neutron and protons individually. If the nuclear reaction rate which produces A out of interactions between Z protons and (A-Z)neutrons exceeds the expansion rate of the Universe, we maintain a chemical equilibrium. In this equilibrium the chemical potentials are related by:

$$\mu_A = Z\mu_P + (A - Z)\mu_n \tag{3.2.2}$$

Which can be expressed in terms of neutron and proton number densities, and substituted into 3.2.1 in addition to the binding energy of a nucleon.

$$B_A \equiv Zm_p + (A - Z)m_n - m_A \tag{3.2.3}$$

Then we obtain an expression for the number density of a nucleon.

$$n_A = g_A A^{\frac{3}{2}} 2^{-A} \left(\frac{2\pi}{m_N}\right)^{\frac{3(A-1)}{2}} n_p^Z n_n^{A-Z} \exp\left(\frac{B_A}{T}\right) \tag{3.2.4}$$

It is useful to introduce the notation $n_N = n_n + n_p + \sum_i (A_i n_{A_i})$ for this section, as the number fraction contributed by a specific nuclear species A(Z) is defined as:

$$\begin{aligned} X_A &= \frac{n_A A}{n_N} \\ \sum_i X_i &= 1 \end{aligned} \tag{3.2.5}$$

This fraction of a nucleon A(Z) in NSE is then found to be:

$$\begin{aligned} X_A =& g_A[\zeta(3)^{A-1} \pi^{\frac{(1-A)}{2}} 2^{\frac{3A-5}{2}}] A^{\frac{5}{2}} \left(\frac{T}{m_N}\right)^{\frac{3(A-1)}{2}} \\ &\times \eta^{A-1} X_p^Z X_n^{A-Z} \exp\left(\frac{B_A}{T}\right) \end{aligned} \tag{3.2.6}$$

Where $\zeta(3) \simeq 1.2$ is the Riemann-zeta function, and $\eta \equiv \frac{n_N}{n_\gamma}$ is the ratio between the number of nucleons to the number of photons per comoving volume. We will

now examine the initial conditions, and then consider the conditions necessary for production of light elements during nucleosynthesis:

- Inital conditions ($T \gg 1$MeV, $t \ll 1$ sec): The ratio between the two nucleons, the proton and the neutron, is crucial to the accuracy of the model as the production of the ^4He abundances absorb virtually all neutrons. Thus interactions which exchange neutron and proton numbers (weak interactions)

$$\begin{aligned} n &\leftrightarrow p + e^- + \bar{\nu}_e \\ n + \nu_e &\leftrightarrow p + e^- \\ n + e^+ &\leftrightarrow p + \bar{\nu}_e \end{aligned} \tag{3.2.7}$$

  are of high importance as they maintain the thermal equilibrium between the two nucleons species. By comparing the weak interaction rate against the Hubble expansion parameter we can determine when these interactions fall out of equilibrium. From [7] eq.(4.19) we can write a simple expression which holds for $T \gtrsim m_e$:

$$\frac{\Gamma_{weak}}{H} \sim \frac{T}{0.8\text{MeV}} \tag{3.2.8}$$

  This equation implies that at temperatures above 0.8 MeV, we can expect the ratio between the nucleons to mirror the equilibrium values of $X_n \simeq X_p$. Since the reaction rates for nuclear reactions above $T \sim 1$ MeV are also larger than the expansion rate one can maintain a nuclear statistical equilibrium. For values closer to and below 0.8 MeV, the weak interactions fall out of equilibrium and one expects to to generate an asymmetry in the nucleon numbers. The fact that the nucleons did not coalesce into the light elements until low temperatures can be attributed to nuclei with large binding energy, e.g. ^{4}He and ^{12}C , do not fall into equilibrium abundance of unity until the temperature reaches $T \sim 0.3$ MeV and the high entropy of the system,$\eta \ll 1$.

- $T = 10$MeV, $t = 10^{-2}$ sec : The epoch is dominated by radiation and takes place before the decoupling of the neutrinos from the heat bath and the subsequent annihilation of e^+e^-. Additionally in this epoch the weak interaction rates are significantly larger than the expansion rate H, which means the ratio between the neutrons and protons $\frac{n}{p}$ closely matches the

equilibrium value of 1. The lighter elements, e.g. ^{3}He , fall into NSE but the abundances are extremely small. This follows from the small value of $\eta = 10^{-9}$ and means that the NSE is dominated by neutrons and protons.

$$\begin{aligned} X_n, X_p &\simeq 0.5 \\ X_i &= \mathcal{O}(10^{-12} \sim 10^{-126}) \end{aligned} \tag{3.2.9}$$

- $T \simeq 1$MeV, $t = 1$ sec : As the Universe moves towards this temperature the neutrinos decouple from the heat bath and shortly after the e^+e^- annihilate, this causes the entropy of the photons to increase significantly. This entropy transfer causes a relative temperature increase of the photons to the neutrinos by a factor of $(11/4)^{1/3}$. As the temperature lowers even more, weak interactions freeze out (interaction rate lower than the expansion rate of the Universe, $\frac{\Gamma_{weak}}{H} < 1$) and the ratio between neutrons and protons reaches an equilibrium value of $(n/p)_{\text{freeze out}} \simeq \frac{1}{6}$. As in the first epoch, the light nuclear species still have small abundances compared to the number density of the neutrons and protons in NSE. As the weak interactions are still present but heavily suppressed, the ratio decreases of n/p from 1/6 to 1/7.

$$\begin{aligned} X_p &\simeq \frac{1}{7} \\ X_n &\simeq \frac{6}{7} \\ X_i &\simeq \mathcal{O}(10^{-12} \sim 10^{-108}) \end{aligned} \tag{3.2.10}$$

- $T = 0.1 \sim 0.3$ MeV , $t = 1$ to 3 minutes : As the Temperature of the heat bath approches 0.3 MeV, the ^{4}He mass fraction becomes close to unity. But the rate of the production of ^{4}He is mainly limited by two factors: the colomb-barrier suppression becomes significant at this temperature, and the number density of D, ^{3}He and ^{3}H which fuel the production are so small at T$\sim$ 0.5 MeV. This causes the density to fall below the NSE value. It is first at T$\sim$ 0.1 MeV that the abundances of these fuels are high enough to maintain the NSE abundance of ^{4}He. By the time the abundance of ^{4}He becomes significant, the coulomb-barrier suppression comes such a factor that despite the binding energy of ^{12}C and ^{16}O being higher than ^{4}He, the nucleosynthesis of these elements is suppressed significantly. But there is some production of Li which is valuable in determining limits on

nucleosynthesis, as its production is strongly effected by abundances of D and ^{4}He.

The accuracy that BBN provides is responsible for some of the strongest bounds on allowed masses/lifetimes for baryogenesis, and is especially sensitive to the charge of these particles. Problematically for this thesis, the potential Stau NLSP can create bound states with the heavier elements, e.g. $^4\mathrm{He}\tau^-$, which can cause problems with overproduction of heavier elements if the lifetime is large enough[9, 10]. The mechanism responsible for the overproduction is only possible in Catalyzed BBN (CBBN), in which bound states between massive negatively charged particles X^- and light nuclei is allowed. ^{6}Li has in Standard BBN (SBBN) a cross section of the interaction D+^{4}He$\rightarrow \gamma+^6$Li, which is strongly suppressed compared to the other diagrams in SBBN as a result of the production of a final state photon. In CBBN, the interaction of D+^{4}HeX$^- \rightarrow \mathrm{X}^-+^6$Li does not have a final state photon as it is absorbed by the charged particle, which manifests itself as a significant increase in the cross section of the order $\mathcal{O}(10^7)$ compared to the SBBN case. The BBN bounds are included in all Graphs below to determine the viability of the NLSP candidate.

3.3 Baryogenesis

There are three basic conditions required to generating a baryon asymmetry from an initially baryon symmetric state[7]:

- Baryon number violating processes: Naturally we want interactions which produce some asymmetry between baryons and anti-baryons. If not the current asymmetry would only reflect the initial asymmetry in the universe.
- Charge Parity and Charge violating processes: Without C and CP violating processes inducing a preference for baryons or anti baryons, the B-non-conserving reactions would produce baryons and anti-baryons at the same rate. Thus there will be no produced asymmetry baryon number. To remedy this we have to include C and CP violating processes.
- Non-equilibirum interactions: While in thermal equilibrium, reactions which produce asymmetry has an equal probability of being reversed because of CPT conservation. As such an additional condition is that the

reactions which produce this asymmetry fall out of equilibrium, i.e. the reaction rate is less than the expansion rate of the universe. This effectively means that in the regime $\frac{\Gamma}{H} < 1$, the particles are less likely to pair-annihilate and washing out produced asymmetry.

Leptogenesis is one such process which might be used to generate such an asymmetry in the early universe. The sphaleron processeses, already present in SM, are responsible for the baryon number violation. Non equilibrium decays can arise from the expansion of the universe which is present in standard cosmology. Finally the massive right handed neutrinos' weak interactions violate both C and CP.

3.4 Leptogenesis

Central to baryogenesis is the mechanism of asymmetry production [11].

$$\eta_B = \frac{Y_B - Y_{\bar{B}}}{Y_\gamma} \tag{3.4.1}$$

This asymmetry is given by Y_B, $Y_{\bar{B}}$ and Y_γ, which are the baryon, anti-baryon and photon abundances respectively. The mechanism of thermal Leptogenesis is an effective way of producing such an asymmetry. Leptogenesis' strength lies in the CP violating interaction of the heavy, right handed, majorana neutrinos, which is the massive partners of the left handed neutrinos. When these massive partners decay, as a result of their majornana nature they do not conserve lepton number. Additionally sphaleron processes, which violate B+L (baryon + lepton number) result in non-conservation of baryon number. As such an asymmetry in the lepton number can be transferred to an asymmetry in the baryon number. Neglecting the asymmetry production caused by the decay of $N_{2,3}$ (simplified thermal Leptogenesis) the Boltzmann equations for the system can be written as follows:

$$\frac{dN_{N_1}}{dz} = -(D+S)(N_{N_1} - {N^{eq}}_{N_1}) \tag{3.4.2}$$

$$\frac{dN_{B-L}}{dz} = -\epsilon_1 D(N_{N_1} - {N^{eq}}_{N_1}) - W N_{B-L} \tag{3.4.3}$$

Where $z = \frac{M_1}{T}$, and D & S are the decay and scattering rates per co-moving volume.

$$D, S = \frac{\Gamma_{D,S}}{(Hz)} \tag{3.4.4}$$

In addition the amount of right handed neutrinos and B-L asymmetry are given as N_{N_1} and N_{B-L}. These quantities are all given for a comoving volume containing one photon. The Hubble parameter is given by:

$$H \simeq \sqrt{\frac{8\pi^3 g_*}{90}} \frac{M_1^2}{M_{Pl}} \frac{1}{z^2} \approx 1.66 g_* \frac{M_1^2}{M_{Pl}} \frac{1}{z^2} \tag{3.4.5}$$

Where $g_* = g_{SM} = 106.75$ is the total number of degrees of freedom, and $M_{Pl} = 1.22 \times 10^{19}$GeV is the Planck mass. The degrees of freedom from N_1 are disregarded, because in the preferred regime of strong washout the right handed neutrinos are non-relativistic. An important variable of Leptogenesis is how quickly the asymmetry is allowed to efficiently be brought into equilibrium by the washout processes. To determine if the washout is strongly or weakly forcing the decay into an equilibrium state, we introduce a decay parameter K [11].

$$K = \frac{\Gamma_D(z=\infty)}{H(z=1)} = \frac{\widetilde{m}_1}{m_*} \tag{3.4.6}$$

We can find the effective neutrino mass form formulas similar to the ones found with the seesaw mechanism, but for fixed M_1, as the other more massive neutrinos are disregarded in the simple model of Leptogenesis.

$$\widetilde{m}_1 = \frac{\left(m_D^\dagger m_D\right)_{11}}{M_1} \tag{3.4.7}$$

Where $\widetilde{m}_1$ can be shown to fall within the range of $m_1 \leq \widetilde{m}_1 \leq m_3$ [12]. With the equilibrium neutrino mass of the order:

$$m_* = \frac{16\pi^{5/2}\sqrt{g_*}}{3\sqrt{5}} \frac{v^2}{M_{Pl}} \simeq 1.08 \times 10^{-3}\text{eV} \tag{3.4.8}$$

The B-L asymmetry that remains when N_1 freezes out can be converted into the baryon asymmetry.

$$\eta_B = \frac{a_{sph}}{f} N_{B-L}^f \tag{3.4.9}$$

Where $a_{sph} = \frac{28}{79}$ amount of B-L asymmetry transferred to baryon asymmetry by sphaleron processes, $f = \frac{2387}{86}$ is the dilution factor by production of photons during Leptogenesis and N_{B-L}^f is the final value for the B-L asymmetry produced during Leptogenesis. N_{B-L}^f can also be expresssed as[11]:

$$N_{B-L}^f = \frac{3}{4} \epsilon_1(M_1, \bar{m}_1^2) \kappa_f(\tilde{m}_1, M_1, \bar{m}_1^2) \tag{3.4.10}$$

where ϵ_1 the generated CP asymmetry, and κ_f is efficiency factor. In general one also has to consider how the lepton asymmetry is distributed among the lepton flavours, but the suggested "one flavour" approach with assumed large mixing angles for the left and right handed neutrinos is accurate to $\mathcal{O}(1)$ corrections.

3.5 Timeline of Leptogenesis

Its useful to construct a timeline of events to better get an understanding of at what temperature regimes the different steps of Leptogenesis takes place. T is the temperature of the heatbath and M_1 is the mass of the lightest right handed neutrino.

- T $\gg M_1$: Interactions and decays in the early universe serve to produce some initial abundance of massive right handed neutrinos, where we will only be considering the lightest N_1[11]. As the temperature lowers, N_1 will start to decay and the inverse decays will push it into a thermal equilibrium. These interactions are described by a set of Boltzmann equations in chapter 3.4. The initially produced B-L asymmetry from the N_1 decay is quickly washed out because of the washout interactions, which will be described further in chapter 3.6.

- T$>M_1$: The equilibrium density of N_1 slowly decreases as N_1 slowly become more non-relativistic and the inverse decays less likely as a result of change of temperature.

- T$\simeq M_1$: Around $z \simeq 3-8$, where z is defined as the ratio between neutrino mass and the temperature of the heat bath $\frac{N_1}{T}$, the neutrinos become fully non-relativistic. Therefore the generated B-L asymmetry is less likely to be washed out by inverse decays and scattering interactions (particularly the $\Delta L = 2$) as they are sensitive to the high mass of the N_1. Since this region is where the majority of the asymmetry is produced, we can define $T_B = \frac{M_1}{z \simeq (3-8)}$ as the temperature of Baryogenesis.

- T$<M_1$: At temperatures this low the interactions between N_1 and the heat bath becomes so unlikely that it decouples from the heat bath. As the temperature becomes even lower the neutrinos freeze out, as freeze out occurs as the interaction rate becomes lower than the expansion rate of the universe $\frac{\Gamma}{H} < 1$, and the produced B-L asymmetry becomes fixed.

3.6 Washout

Washout is a collective term for all interactions which reduce and/or change the total asymmetry produced between a particle's decay and freeze out[11]. Since the out of equilibrium decay of a heavy right handed neutrino would produce some asymmetry in the lepton number, the strength of the washout, and how quickly the asymmetry is pushed back into equilibrium, becomes important. From eq.3.4.6 we can determine in which region of washout we are in. For strong washout regime K$\gtrsim 3$ the N_1 decays are quickly brought into equilibrium, and for $K < 1$ we are in the weak washout regime where N_1 is much slower at pushing the system into a equilibrium. We can determine the washout by looking at the $\Delta L = 1, 2$ scattering processes as well as the inverse decay channels to determine how much asymmetry is produced during Leptogenesis. The washout for the right handed heavy neutrino decay process can be separated into two functions describing the behaviour of either decay, inverse decay and $\Delta L = 1$ scatterings dependent on $\tilde{m}_1$ or $\Delta L = 2$ scatterings dependent on the heavy neutrino masses M_1.

$$W(z) = W_o(z; \tilde{m}_1) + \Delta W(z; M_1 \bar{m}^2) \tag{3.6.1}$$

In the low temperature limit $\Delta W(z; M_1 \bar{m}^2)$ becomes expressable as a function of M_1, $\widetilde{m}_1$ and z [11].

$$\Delta W(z; M_1 \bar{m}^2) \simeq \frac{\omega}{z^2} \left(\frac{M_1}{10^{10}\mathrm{Gev}} \right) \left(\frac{\bar{m}}{\mathrm{eV}} \right)^2 \tag{3.6.2}$$

where $\omega \simeq 0.186$ is a dimensionless constant. For values of $z > z_B$ no asymmetry is produced, and we can introduce a dampening factor on the efficiency factor.

$$\bar{\kappa}_f(\tilde{m}_1, M_1 \bar{m}^2) = \kappa_f(\tilde{m}_1) e^{-\int_{z_B}^{\infty} \Delta W dz} \tag{3.6.3}$$

Keep in mind the $\kappa_f(\tilde{m}_1)$ is the efficiency factor in the regime where M_1 is sufficiently small such that the contribution from the ΔW term is negligible. For z_B large enough, we can substitute in the lower energy limit and obtain:

$$\bar{\kappa}_f(\tilde{m}_1, M_1 \bar{m}^2) = \kappa_f(\tilde{m}_1) e^{-\frac{\omega}{z_B}\left(\frac{M_1}{10^{10}\mathrm{Gev}}\right)\left(\frac{\bar{m}}{\mathrm{eV}}\right)^2} \tag{3.6.4}$$

Where z_B is the local minimun for the integral given in the exponential 3.6.3, which generates the peak value for κ_f. Since $z_B = \frac{M_1}{T_B}$ we can interpret T_B as temperature of baryogenesis, the point at which the neutrinos are full non-relativistic.

The decay channels of the extended SM neutrino:

- Decay and inverse decay: $N_1 \leftrightarrow l\phi$, $N_1 \leftrightarrow \bar{l}\bar{\phi}$
- $\Delta L = 1$ scatterings: $N_1 l \leftrightarrow \bar{t}q$, $N_1\bar{l} \leftrightarrow t\bar{q}$, $N_1 t \leftrightarrow \bar{l}q$, $N_1\bar{t} \leftrightarrow l\bar{q}$
- $\Delta L = 2$ scatterings : $ll \leftrightarrow \bar{\phi}\bar{\phi}$, $\overline{ll} \leftrightarrow \phi\phi$ and $l\bar{\phi} \leftrightarrow \bar{l}\phi$

The $\Delta L = 2$ scattering interactions are mediated by the massive right handed neutrinos, and are therefore sensitive to their masses, $M_{1,2,3}$.

For $K \simeq 3$, the strong washout regime, the inverse decays quickly lower temperature of the right handed neutrinos to non-relativistic energies[6]. Additionally, since the decay and inverse decay are so strong, the number of neutrinos quickly fall into equilibrium and washout any initial asymmetry present before Leptogenesis. As a result, the strong washout regime has a negligible dependence on initial conditions. The efficiency factor (3.6.3) is strongly peaked around $z_B \gg 1$, which in turn implies that the majority of the asymetry is produced around the temperature of baryogenesis T_B.

3.7 CP-asymmetry

Charge parity asymmetry is a trait some interactions/decays have, if the possible CP final states have a non equal probability to occur. The CP violation arises from interference of loop diagrams with tree level[13]. These corrections can be assumed to be of the order α^N, where α is the coupling parameter for the loop particles, and N is the number of loops in the lowest order diagram which interferes with tree level to produce $\epsilon \neq 0$. The CP-asymmetry generated by right handed neutrino decays arise from tree level and one order loop corrections of the two final states $l\phi$ and $\bar{l}\bar{\phi}$. Assuming standard mass hierarchy for the massive neutrinos of extended SM, i.e. $M_1 \ll M_{2,3}$, the CP-asymmetry generated by heavy neutrino decay can be expressed as[13, 14]:

$$\epsilon = \frac{\Gamma(N_1 \to l\phi) - \Gamma(N_1 \to \bar{l}\bar{\phi})}{\Gamma(N_1 \to l\phi) + \Gamma(N_1 \to \bar{l}\bar{\phi})} \tag{3.7.1}$$

The maximal asymmetry from N_1 decays can then be found by considering

tree level and lepton-higgs interactions to obtain the simple expression [11, 15]

$$\epsilon_1^{max}(M_1, \tilde{m}_1, m_1) = \frac{3}{16\pi}\frac{M_1}{v^2}(m_3 - m_1) \tag{3.7.2}$$

If one chooses to express $\bar{m}^2$ as a function of m_1, m_{atm} and m_{sol} you can simplify the expression such that for $m_1 = 0$ the maximal CP asymmetry is only dependent on M_1. For $m_1 \geq 0$ we introduce the function $\beta(\tilde{m}_1, m_1) \leq 1$ which is maximized for the limit $\frac{m_1}{\tilde{m}_1} \to 0$.

$$\beta(m_1) = \frac{m_3 - m_1}{m_{atm}} \tag{3.7.3}$$

$$\epsilon_1^{max}(M_1, \tilde{m}_1, m_1) = \epsilon_1^{max}(M_1)\beta(\tilde{m}_1, m_1) \tag{3.7.4}$$

Setting $\beta = 1$ and assuming $m_3 \simeq m_{atm}$:

$$\epsilon_1^{max}(M_1) = \frac{3}{16\pi}\frac{M_1 m_{atm}}{v^2} \tag{3.7.5}$$

where $\kappa_f(\bar{m}_1)$ is the efficiency factor for low M_1 masses where the ΔW term is negligible.

Chapter 4

Limits on entropy production

4.1 Maximal η_B

We now want to find the maximal value of η_B^{max} with respect to M_1[6]. By differentiating $\ln \eta_B$ we obtain the peak value with respect to the heavy neutrino mass:

$$\frac{d \ln \eta_B}{dM_1} = 0 \tag{4.1.1}$$

Using the identity above and Equation (3.4.9), substituting for ϵ_1 and κ_f, we find an expression:

$$\frac{d \ln M_1}{dM_1} - \frac{d\left(\frac{\omega}{z_B}\right)\left(\frac{M_1}{10^{10}\mathrm{Gev}}\right)\left(\frac{\bar{m}}{\mathrm{eV}}\right)^2}{dM_1} = 0 \tag{4.1.2}$$

Which after some simplification yields an equation easily reducible to express M_1

$$\left(\frac{\omega}{z_B}\right)\left(\frac{M_1}{10^{10}\mathrm{Gev}}\right)\left(\frac{\bar{m}}{\mathrm{eV}}\right)^2 = 1 \tag{4.1.3}$$

Solve for M_1, assume $\bar{m}_1 \simeq m_{atm} \simeq m_3$ and $\omega \simeq 0.186$:

$$M_1 = \frac{z_B}{\omega}\left(\frac{\mathrm{eV}}{\bar{m}}\right)^2 10^{10}\mathrm{GeV} = 2 \times 10^{13} z_B \left(\frac{0.05\mathrm{eV}}{m_3}\right)^2 \mathrm{GeV} \tag{4.1.4}$$

Then we substitute this value for M_1 into (3.4.9) to obtain a new expression for η_B^{max}, only dependent on κ, m_3 and z_B:

$$\begin{aligned}\eta_B^{max} &= \frac{a_{sph}}{f}\frac{3}{4}\frac{3}{16\pi}\frac{M_1 m_3}{v^2}\kappa_f(\tilde{m}_1)e^{-\frac{\omega}{z_B}\left(\frac{M_1}{10^{10}\text{Gev}}\right)\left(\frac{\tilde{m}_1}{\text{eV}}\right)^2} \\ &\simeq 10^{-2}\frac{3}{16\pi}\frac{2\times 10^{13}}{176^2}5\times 10^{-11}z_B\left(\frac{0.05\text{eV}}{m_3}\right)\kappa_f(\tilde{m}_1)e^{-0.186\left(\frac{2\times 10^3}{400}\right)} \\ &\simeq 8\times 10^{-6}z_B\kappa_f(\tilde{m}_1)\left(\frac{0.05\text{eV}}{m_3}\right)\end{aligned} \tag{4.1.5}$$

with $v = 174$GeV. Now we can determine how large the range for the baryon asymmetry can be, by considering z_B and κ_f. The value z_B can be found for any given K by the approximation in eq.4.1.6 below[11].

$$z_B \simeq 1 + \frac{1}{2}\ln\left(1 + \frac{\pi K^2}{1024}\left[\ln\left(\frac{3125\pi K^2}{1024}\right)\right]^5\right) \tag{4.1.6}$$

For the upper bound of z_B we find $\widetilde{m}_1 \simeq m_{atm}$ yielding $z_B \simeq 8$. For $\widetilde{m}_1 \simeq m_{sol}$ we find $z_B \simeq 8$. Where the m_{atm} and m_{sol} are the measured masses for atmospheric and solar neutrinos respectively. For the lower limit on strong washout, $K \simeq 3$ $\tilde{m}_1 \simeq 3\times 10^{-3}$eV and $z_B \simeq 3$. This gives a mass range for the max value of M_1, for fixed mass for $m_3 = 0.05$:

$$\begin{aligned}M_1(z_B \simeq 8) &\simeq \mathcal{O}(10^{14})\text{Gev} \\ M_1(z_B \simeq 6) &\simeq \mathcal{O}(10^{14})\text{Gev} \\ M_1(z_B \simeq 3) &\simeq \mathcal{O}(10^{13})\text{Gev}\end{aligned} \tag{4.1.7}$$

Now using figure. 9 in [11] for $M_h \simeq 125$GeV, we find the expected efficiency factors for the given value of $\widetilde{m}_1$.

$$\begin{aligned}\kappa_f(\tilde{m}_1 = m_{atm}) &\simeq 5\times 10^{-3} \\ \kappa_f(\tilde{m}_1 = m_{sol}) &\simeq 3\times 10^{-2} \\ \kappa_f(\tilde{m}_1 = 3\times 10^{-3}\text{eV}) &\simeq 0.17\end{aligned} \tag{4.1.8}$$

The maximal value for for the baryon asymmetry, η_B^{max}, can then be found to have the values:

$$\begin{aligned}\eta_B^{max}(\kappa_f \simeq 5\times 10^{-3}, z_B \simeq 8) &\simeq 6\times 10^{-8} \\ \eta_B^{max}(\kappa_f \simeq 3\times 10^{-2}, z_B \simeq 6) &\simeq 5\times 10^{-7} \\ \eta_B^{max}(\kappa_f \simeq 0.17, z_B \simeq 2) &\simeq 3\times 10^{-6}\end{aligned} \tag{4.1.9}$$

These values differ as expected from the equation given in [8] since they do not take into account the dampening effect of ΔW.

$$\begin{aligned}
&\eta_B^{max}(\kappa_f \simeq 5\times10^{-3}, M_1 \simeq \mathcal{O}(10^{14})\text{GeV}) \simeq 1.3\times10^{-6}\\
&\eta_B^{max}(\kappa_f \simeq 3\times10^{-2}, M_1 \simeq \mathcal{O}(10^{14})\text{GeV}) \simeq 8\times10^{-6}\\
&\eta_B^{max}(\kappa_f \simeq 0.17, M_1 \simeq \mathcal{O}(10^{13})\text{GeV}) \simeq 5\times10^{-6}
\end{aligned} \tag{4.1.10}$$

4.2 Late time entropy production from the baryon asymmetry

To determine the entropy production generated between the decay of the heavy neutrino and the surface of last scattering, we compare the asymmetry measured from the Cosmic Microwave Background Radiation and the ones found in the previous section. The η_B^{CMBR} is found experimentally and becomes the lower bound on allowed CP asymmetry[6].

$$\eta_B^{CMBR} = (6.3 \pm 0.3)\times10^{-10} \tag{4.2.1}$$

The asymmetry is reduced by a factor of Δ, the entropy dilution factor, from the peak of asymmetry produced until the current measurable value of η_B^{CMBR}.

$$\eta_B^{peak} = \Delta^{-1}\eta_B^{CMBR} \tag{4.2.2}$$

This does also strictly imply there exists a lower bound on the entropy production after the heavy neutrinos have decayed in the early universe, if one found $\eta_B^{CMBR} = \eta_B^{peak}$ then there is no entropy production present. In addition since there are no mechanisms to account for negative entropy generation, this condition becomes the lower bound on entropy production. We can now find the entropy measure Δ by using eq. 3.1.7.

$$\begin{aligned}
\Delta_{sol} &= \frac{\eta_B^{max}(\kappa_f \simeq 5\times10^{-3}, z_B \simeq 8)}{\eta_B^{CMBR}} \simeq \frac{6\times10^{-8}}{6.3\times10^{-10}} \simeq 10^2\\
\Delta_{atm} &= \frac{\eta_B^{max}(\kappa_f \simeq 3\times10^{-2}, z_B \simeq 6)}{\eta_B^{CMBR}} \simeq \frac{5\times10^{-7}}{6.3\times10^{-10}} \simeq 8\times10^3\\
\Delta_{peak} &= \frac{\eta_B^{max}(\kappa_f \simeq 0.17, z_B \simeq 2)}{\eta_B^{CMBR}} \simeq \frac{3\times10^{-6}}{6.3\times10^{-10}} \simeq 5\times10^4
\end{aligned} \tag{4.2.3}$$

The Δ_{peak} value matches well with the assumption stated in [8], which found the upper bound of $\Delta < 2\times10^4$ for the case of hirarical neutrinos and $M_1 > 4\times10^{13}$.

Keep in mind the equation used to calculate these values in reference [8] uses a linear approximation, and as such does not take into account the dampening factor from washout from eq. 3.6.4, and is therefore inaccurate for Δ_{sol} and Δ_{atm} when considering the strong washout regime.

4.3 MSSM extension of Leptogenesis

When going from extended SM to the Minimal Supersymmetric Standard Model there are a couple of problems we need to consider. Firstly, by adding the supersymmetric parter of the massive right handed neutrino, the sneutrino, we need to consider the new decay, inverse decay and $\Delta L = 1, 2$ interactions for the sneutrino that could produce a lepton asymmetry. Supplementary decay processes such as $\tilde{N} \to \tilde{\phi} l$ or $\tilde{N} \to \tilde{\phi}^* \bar{l}$ also contribute to the lepton asymmetry; chapter 4.3.1 includes these decay and inverse decays. Secondly, we have to look at the already existing interactions that generate CP-asymmetry[14], for example MSSM corrections to $N \to l\phi$ seen in the fig.4.3.1.

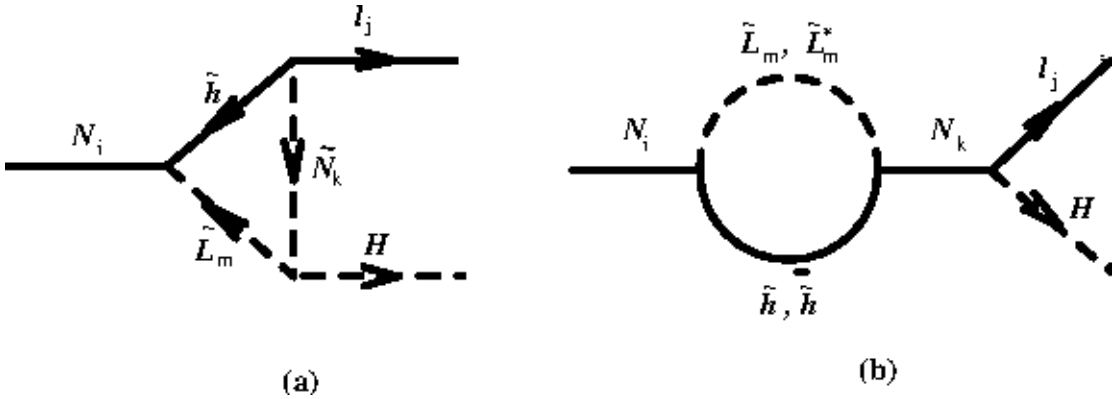

Figure 4.3.1: Supersymmetric corrections to the decay $N_1 \to lH$ which contributes to the genetration of CP asymmetry. Taken from ref.[14]

The immediate problem is that the washout terms $\Delta L = 1, 2$ become strictly harder to compute, especially since the technique of separating into terms proportional to $\tilde{m}_1$ and M_1 becomes difficult. This is because the additional washout processes may include further mixing between the MSSM particles not present in SM. Since we wish to avoid such complications, we chose a simple

extension by assuming that the washout in the MSSM extension is identically separable just like in SM.

$$\begin{aligned} W(z) &= W_{SM}(z;\tilde{m}_1, M_1) + W_{Extended}(z;\tilde{m}_1, \tilde{M}_1) \\ &= W_o(z;\tilde{m}_1) + \Delta W(z;M_{N_1}) + \Delta W(z;M_{\tilde{N}_1}) \end{aligned} \tag{4.3.1}$$

Keep in mind that the ΔW terms describe the individual $\Delta L = 2$ interactions for both the sneutrino and the neutrino with no interference terms, i.e. we assume that for at large temperatures the $\Delta L = 2$ loop corrections are negligible. Additionally, we can predict that the washout will act similarly at low temperatures, the interactions which dominate in SM also similarly dominate for the extension into MSSM. As such, the approximation used in 3.6.2 can hold for the sneutrino washout as well. We now extend the efficiency factor, from eq.3.6.3, with an additional term in the dampening factor for the sneutrino.

$$\bar{\kappa}_f(\tilde{m}_1, M_1\bar{m}^2) = 2\kappa_f(\tilde{m}_1)e^{-\int_{z_B}^{\infty}\Delta W_{N_1}+\Delta W_{\tilde{N}_1}dz} \tag{4.3.2}$$

We will assume that κ_f for low energies, where the ΔW terms are negligible, will be increased by a factor 2 directly following from the relation between decay width of the neutrino and sneutrino, $\Gamma_N = \Gamma_{\tilde{N}}$. This equality demands that the $\Delta L = 1$ interactions are of the same order for both the sneutrino and the neutrino. By also assuming that the masses of the neutrinos are equal, since the supersymmetric corrections are small compared to their mass, $m_{N_1} \approx m_{\tilde{N}_1}$,we can simplify eq.4.3.2 [16].

$$\bar{\kappa}_f(\tilde{m}_1, M_1\bar{m}^2) = 2\kappa_f(\tilde{m}_1)e^{-2\frac{\omega}{z_B}\left(\frac{M_1}{10^{10}\mathrm{Gev}}\right)\left(\frac{\bar{m}}{\mathrm{eV}}\right)^2} \tag{4.3.3}$$

Now that we have an expression for the efficiency factor, the next problem is the CP asymmetry. With the extention into MSSM, we introduce new correctional terms to the already existing decays as seen in figure 4.3.1, as a consequence we also must consider the diagrams leading to CP-violation from the sneutrino decay[14].

$$\begin{aligned} \tilde{\epsilon}_l^N &= \frac{\Gamma_{Nl} - \Gamma_{N\bar{l}}}{\Gamma_{Nl} + \Gamma_{N\bar{l}}}, \quad \tilde{\epsilon}_{\tilde{L}^*}^N = \frac{\Gamma_{N\tilde{L}} - \Gamma_{N\tilde{L}^*}}{\Gamma_{N\tilde{L}} + \Gamma_{N\tilde{L}^*}} \\ \tilde{\epsilon}_l^{\tilde{N}^*} &= \frac{\Gamma_{\tilde{N}^*l} - \Gamma_{\tilde{N}\bar{l}}}{\Gamma_{\tilde{N}^*l} + \Gamma_{\tilde{N}\bar{l}}}, \quad \tilde{\epsilon}_{\tilde{L}}^{\tilde{N}} = \frac{\Gamma_{\tilde{N}\tilde{L}} - \Gamma_{\tilde{N}^*\tilde{L}^*}}{\Gamma_{\tilde{N}\tilde{L}} + \Gamma_{\tilde{N}^*\tilde{L}^*}} \end{aligned} \tag{4.3.4}$$

where the first two equation takes care of the CP asymmetry generated by N_1 decays, and the remaining two the $\tilde{N}_1$. It is beneficial to express the total

CP-asymmetry:

$$\tilde{\epsilon}_i = \tilde{\epsilon}_l^{N_i} + \tilde{\epsilon}_{\tilde{L}^*}^{N_i} + \tilde{\epsilon}_l^{\tilde{N}_i^*} + \tilde{\epsilon}_{\tilde{L}}^{\tilde{N}_i} = 4\tilde{\epsilon}_l^{N_i} \tag{4.3.5}$$

Where $\tilde{\epsilon}_l^{N_i} = 2\epsilon_i^{N_i}$ is taken from the SM asymmetry calculation. Now that we have both of these measures, we can use eq 3.4.9 to calculate a new value for the baryon asymmetry, but first we have to calculate the new peak mass for M_{N_1} using eq 4.1.2.

$$M_{N_1}^{MSSM} = \frac{1}{2} M_{N_1}^{SM} \tag{4.3.6}$$

This luckily enough cancels the factor of 2 added to the exponential in eq. 4.3.3 so the total efficiency factor for MSSM gains a factor of 2, $\kappa^{MSSM} = 2\kappa^{SM}$. Keep in mind, we also gain a factor of $\frac{1}{2}$, because of $\eta_B = \frac{n_B}{s}$, as the entropy density s is dependent on g_* which is twice as large for MSSM, $g_*^{MSSM} = 2g_*^{SM}$. We now substitute these into 3.4.9 to obtain the MSSM values for the baryon asymmetry.

$$\begin{aligned}
\eta_B^{MSSM} &= \frac{1}{2}\frac{a_{sph}}{f}\frac{3}{4}\epsilon_1^{MSSM}(M_1^{MSSM})\kappa_f^{MSSM}(\tilde{m}_1)e^{-2\frac{\omega}{z_B}\left(\frac{M_1^{MSSM}}{10^{10}\text{Gev}}\right)\left(\frac{\tilde{m}}{\text{eV}}\right)^2} \\
&= \frac{1}{2}\frac{a_{sph}}{f}\frac{3}{4}8\epsilon_1^{SM}(\frac{M_1^{SM}}{2})2\kappa_f^{SM}(\tilde{m}_1)e^{-2\frac{\omega}{z_B}\left(\frac{M_1^{SM}}{2\times 10^{10}\text{Gev}}\right)\left(\frac{\tilde{m}}{\text{eV}}\right)^2} \\
&= 4\eta_B^{SM}
\end{aligned} \tag{4.3.7}$$

So to find the corrected dilution factor Δ^{MSSM} for the MSSM extension, we substitute into eq.3.1.7.

$$\begin{aligned}
\Delta_{sol} &= \frac{4\times\eta_B^{max}(\kappa_f \simeq 5\times 10^{-3}, z_B \simeq 8)}{\eta_B^{CMBR}} \simeq \frac{24\times 10^{-8}}{6.3\times 10^{-10}} \simeq 4\times 10^2 \\
\Delta_{atm} &= \frac{4\times\eta_B^{max}(\kappa_f \simeq 3\times 10^{-2}, z_B \simeq 6)}{\eta_B^{CMBR}} \simeq \frac{20\times 10^{-7}}{6.3\times 10^{-10}} \simeq 3\times 10^4 \\
\Delta_{peak} &= \frac{4\times\eta_B^{max}(\kappa_f \simeq 0.17, z_B \simeq 2)}{\eta_B^{CMBR}} \simeq \frac{12\times 10^{-6}}{6.3\times 10^{-10}} \simeq 2\times 10^5
\end{aligned} \tag{4.3.8}$$

Further discussion of the assumptions used in this chapter are included in Appendix A.

4.3.1 MSSM spesific interactions

The new interactions from extending to MSSM include the decay channels for $\tilde{N}_1$, and introduce additional decay terms to N_1 decays:

- Decay and inverse decay for $\tilde{N}_1$: $\tilde{N}_1 \leftrightarrow \tilde{l}\phi$, $\tilde{N}_1 \leftrightarrow l\tilde{\phi}$, $\tilde{N}_1 \leftrightarrow \tilde{l}^*\bar{\phi}$, $\tilde{N}_1 \leftrightarrow \bar{l}\tilde{\phi}^*$
- Decay and inverse decay for N_1: $N_1 \leftrightarrow l\phi$, $N_1 \leftrightarrow \tilde{l}\tilde{\phi}$, $N_1 \leftrightarrow \bar{l}\bar{\phi}$, $N_1 \leftrightarrow \tilde{l}^*\tilde{\phi}^*$

We also gain new interactions in the $\Delta L = 1, 2$ processes similar to the ones added in the decays and inverse-decays.

4.4 Stau relic density calculations

Within MSSM one usually considers two different candidates for the Next Lightest Supersymmetric Particle (NLSP), the stau $\tilde{\tau}$ and the lightest neutralino χ_1^0. In this thesis we will only consider the stau candidate. By using the numerical package micrOMEGAs to calculate the Ω_0 we can find the expected relic abundance for the stau measured today for $\Delta = 1$ as micrOMEGAs does not consider entropy production scenarios. [17]. The main stau decay we care about is the $\tilde{\tau} \to \tau\Psi_{3/2}$ channel, since it gives us an easy way to calculate the lifetime of the stau from only a few parameters, specifically $m_{3/2}$ and $m_{\tilde{\tau}}$[18].

$$\Gamma_{\tilde{\tau}}^{\text{2-Body}} = \frac{m_{\tilde{\tau}}^5}{48\pi m_{3/2}^2 M_{Pl}} \times \left(1 - \frac{m_{3/2}^2}{m_{\tilde{\tau}}^2}\right)^4 \tag{4.4.1}$$

Where M_{Pl} is the reduced planck mass, $m_{3/2}$ is the mass of the gravitino and $m_{\tilde{\tau}}$ is the mass of the stau. This requires terms dependent on m_τ to be negligible compared to the mass of the gravitino , $m_{3/2}$. We can now find a value of the lifetime for this interaction by using the simple relation $\tau_{\tilde{\tau}}^{\text{2-Body}} = \frac{1}{\Gamma_{\tilde{\tau}}^{\text{2-Body}}}$.

Chapter 5

Stau NLSP

5.1 Lifetime considerations

Since the lifetime of the stau is sensitive to the gravitino mass we can locate a region which ensures that the decays do not happen late enough to impact the aboundances of hadronic elements created during BBN. By using bounds found in ref [9] for stau masses of the order 300GeV, using eq. 4.4.1 to calculate the gravitino lifetime and finally converting from relic density of stau $\Omega_{\tilde{\tau}}$ to the abundance $Y_{\tilde{\tau}}$ using eq. 5.1.1 [19], we can determine which combinations of yields and lifetimes which can be excluded from BBN considerations.

$$\Omega_\chi h^2 = \frac{s(T_0)h^2}{\rho_c} M_\chi Y_\chi(T_0) = 2.742 \times 10^8 \frac{M_\chi}{GeV} Y_\chi(T_0) \tag{5.1.1}$$

where s is the current entropy density, h is the uncertainty in the Hubble rate and χ denotes the particle species considered. It is important to note that this equation only holds for $Y_\chi \equiv \frac{n_\chi}{s}$. Where as the equation under is valid for $Y'_\chi \equiv \frac{n_\chi}{n_\gamma}$:

$$\Omega_\chi h^2 = 2.742 \times 10^8 \frac{M_\chi}{GeV} Y_\chi(T_0) = 3.91 \times 10^7 \frac{M_\chi}{GeV} Y'_\chi(T_0) \tag{5.1.2}$$

Where the s in $Y_{\tilde{\tau}}$ is the entropy density after $e^\pm$ annihilation-epoch, $s \approx 7n_\gamma$. The biggest constraint on $Y_{\tilde{\tau}}$ is the overproduction of ^{6}Li from the larger masses of the gravitino. For the lower masses, the main constrain on the abundance is the $p \leftrightarrow n$ conversion which is sensitive to pion density, produced through tau decays.

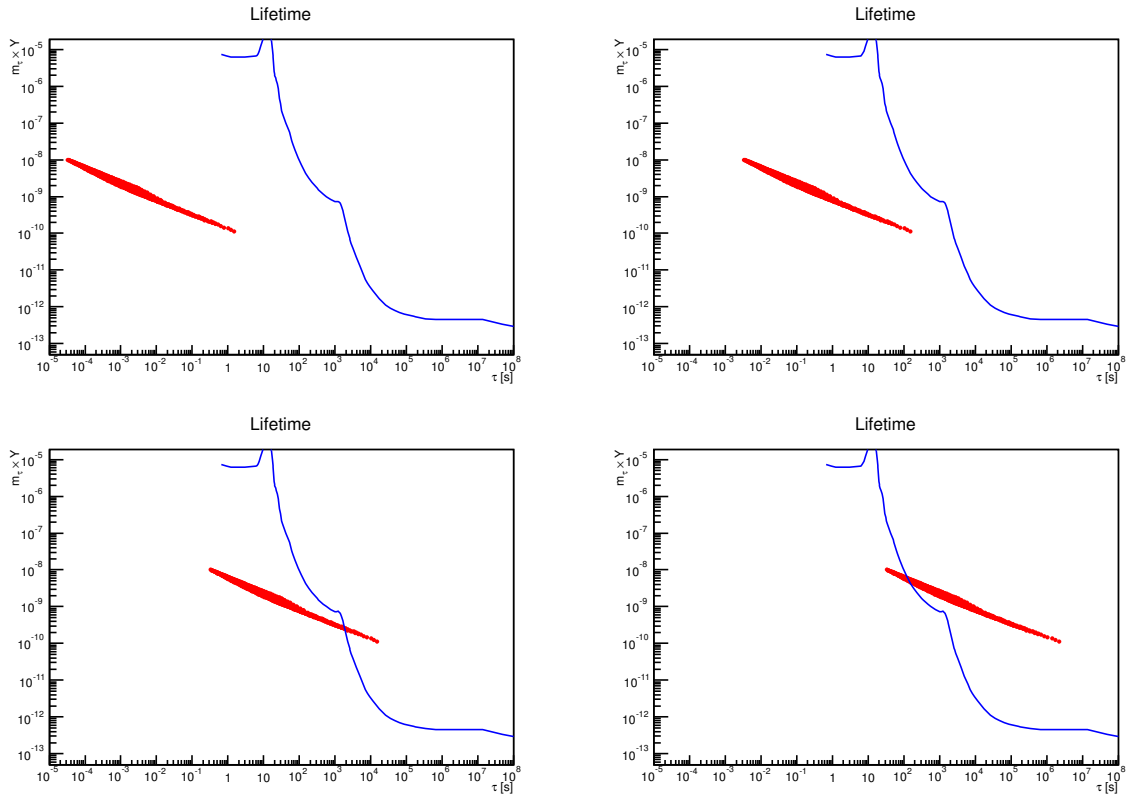

Figure 5.1.1: Graphs with yields found by micrOMEGAs' against the lifetime found from eq.4.4.1 for fixed gravitino mass (plotted from left to right) 0.1GeV, 1GeV, 10GeV and 100GeV. Any point of the generated set (red) which falls above or to the right of the BBN bounds (blue) are not viable as candidates for NLSP.

We now plot the relic density of the stau $\Omega_{\tilde{\tau}}$ against the lifetime of the stau $\tau_{\tilde{\tau}}$, using micrOMEGAs to calculate the relic density of the stau. To obtain these values, we constructed 700 generic MSSM models with the stau as the choice for NLSP, which micrOMEGAs uses to determine decay widths of the MSSM particles. It can then use these widths in addition to a set of Boltzmann equations, as well as the interactions included in the generic MSSM models, to determine the relic densitites.[17].

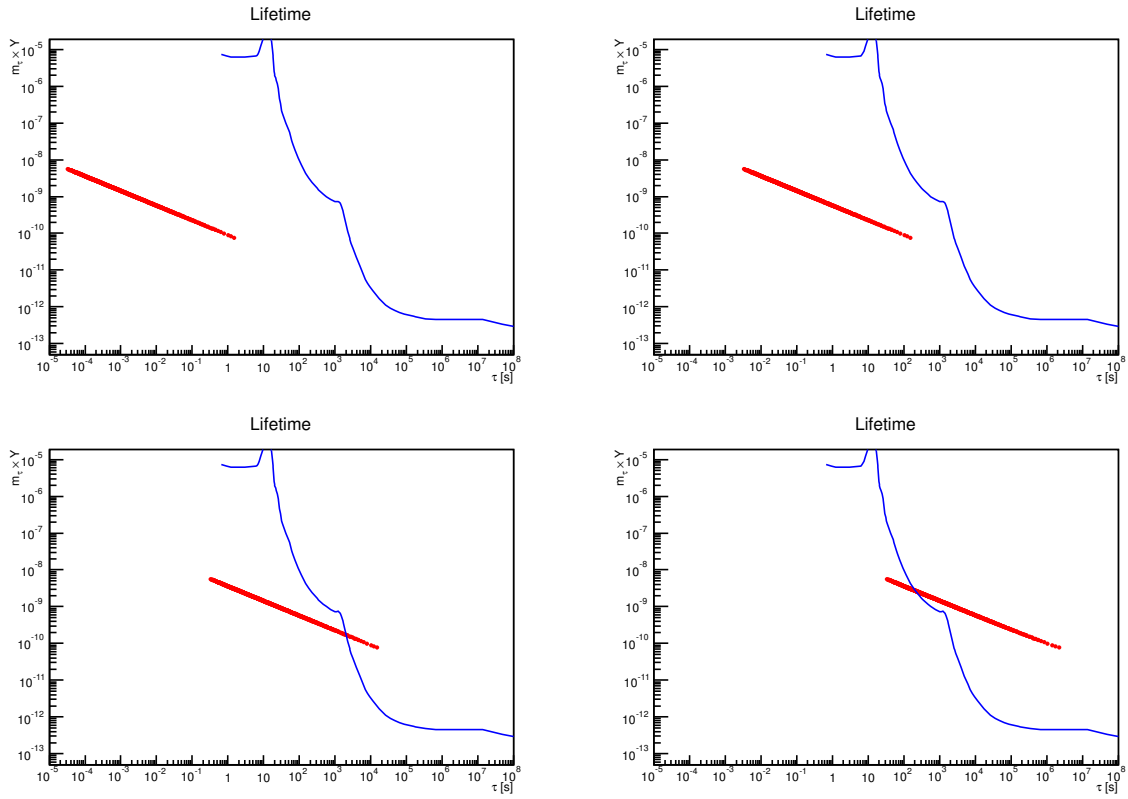

Figure 5.2.1: Graphs with yields found by using eq.5.2.1 against the lifetime found from eq.4.4.1 for fixed gravitino mass (plotted from left to right) 0.1GeV, 1GeV, 10GeV and 100GeV.Any point of the generated set (red) which falls above or to the right of the BBN bounds (blue) are not viable as candidates for NLSP.

5.2 Checking stau yields

With these plots we now compare the values to additional approximations found in reference [9] and [20]. The yields found in [9], gives us a simple linear approximation.

$$Y_{\tilde{\tau}} \simeq 7 \times 10^{-14} \times \left(\frac{m_{\tilde{\tau}}}{100\text{GeV}}\right) \tag{5.2.1}$$

The values found using this approximation matches fairly well with the values calculated from micrOMEGAs. The variance of the abundance in the values generated from micrOMEGAs is larger as the equation only linearly associates the stau mass to the abundance. The relation in [20] is sensitive to wether the

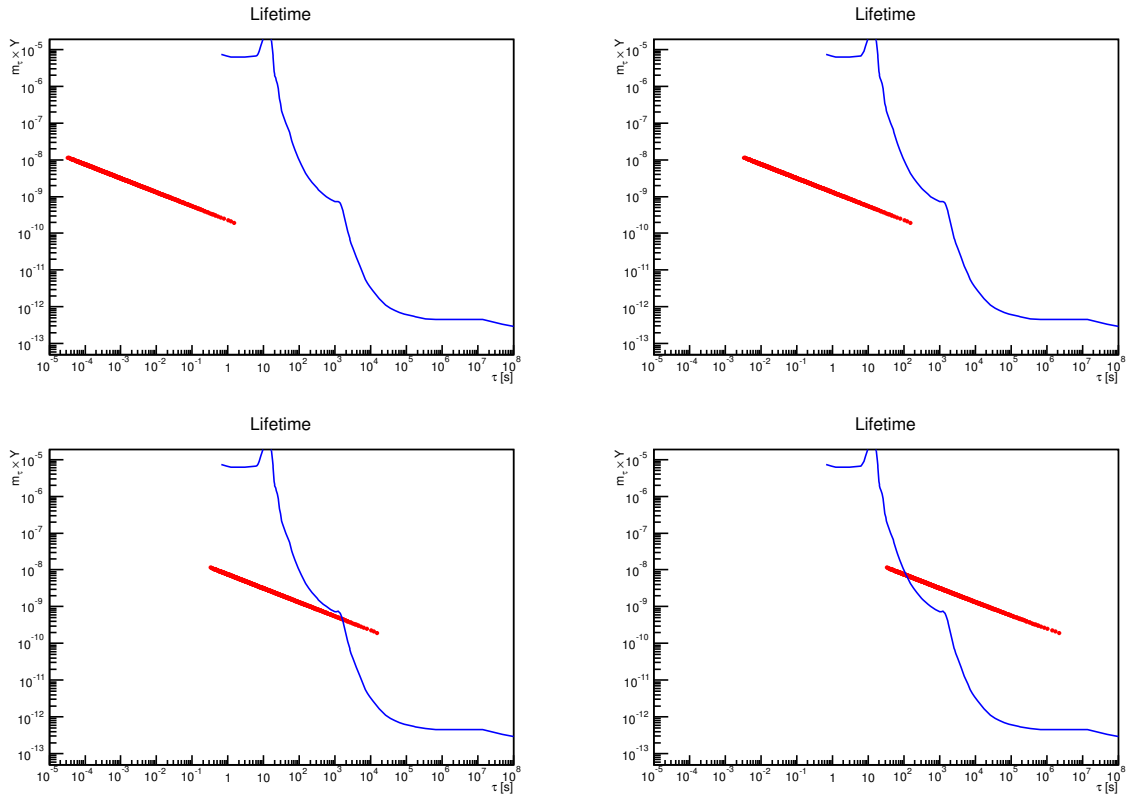

Figure 5.2.2: Graphs with yields found by using eqs.5.2.2 against the lifetime found from eq.4.4.1 for fixed gravitino mass (plotted from left to right) 0.1GeV, 1GeV, 10GeV and 100GeV. Any point of the generated set (red) which falls above or to the right of the BBN bounds (blue) are not viable as candidates for NLSP.

stau is left or right handed, as such we have two relations to plot:

$$\begin{aligned} Y_{\tilde{\tau}_1=\tilde{\tau}_R} &= 1.59 \times 10^{-12} \left(\frac{m_{\tilde{\tau}_1}}{1\text{TeV}}\right)^{0.9} \\ Y_{\tilde{\tau}_1\simeq\tilde{\tau}_L} &= 1.07 \times 10^{-12} \left(\frac{m_{\tilde{\tau}_1}}{1\text{TeV}}\right)^{0.9} \end{aligned} \tag{5.2.2}$$

These values are yet again accurate to the generated micrOMEGAs set, but do map more closely than the simple approximation.

5.3 Plots using gaugino - NLSP mass relation

The next challange is finding a lower bound on the gravitino mass as a function of the stau mass. One can find one such lower bound by looking at the mechanism of gaugino mediation. Since the lower bound found for the gaugino mass has to be strictly larger than the NLSP mass, we can use this lower bound for the stau[21].

$$\left(\frac{m_{3/2}}{m_{1/2}}\right)_{min} = \frac{8\pi\sqrt{C}}{\sqrt{3}\ell_D}\left(\frac{M_4}{M_c}\right)^{\frac{D-4}{D-2}} \tag{5.3.1}$$

Here, D is the number of extra dimensions above the energyscale Λ, ℓ_D is a constant depending on the number of extra dimensions and M_c is mass scale for compactification. This equation gives us a tool to relate the mass of the gravitino, $m_{3/2}$, with the mass of the gaugino, $m_{1/2}$, in such a way that we can better determine the lifetime of the stau by substituting into eq.4.4.1. We will now consider how choice of D and M_c affects the lifetime.

5.3.1 Stau yields for D=5

For the region we are interested in we choose M_c in the order of GUT scale $10^{16} \sim 2 \times 10^{16}$, with the chosen color red in Fig.5.3.1 to Fig.5.3.6. For this region, the values of $\left(\frac{m_{3/2}}{m_{1/2}}\right)_{min}$ corresponds to a range from 0.22 to 0.28. Compared to lifetime generated by eq. 4.4.1, the range of lifetimes is much smaller, and the range falls in the region of larger lifetimes $10^4 \sim 10^6$ seconds. Additionally, of the points fall outside of the BBN bounds before adjusting for entropy production, clearly visible in Fig.5.3.1,Fig.5.3.2 and Fig.5.3.3.

After adjusting for entropy production, Shown in Fig.5.3.4 to Fig.5.3.6, show the majority of points for $\Delta \simeq 2 \times 10^5$ still fall outside the allowed region for BBN. The generated set from micrOMEGAs does not fall below the boundry in the range of allowed values of lifetimes found from eq. 5.3.1. This is problematic, as this is for the case of maximally allowed entropy production for MSSM allowed by the method derived in this thesis. The two other approximations do not benefit significantly from the entropy production either, and do also fall outside of the allowed region.

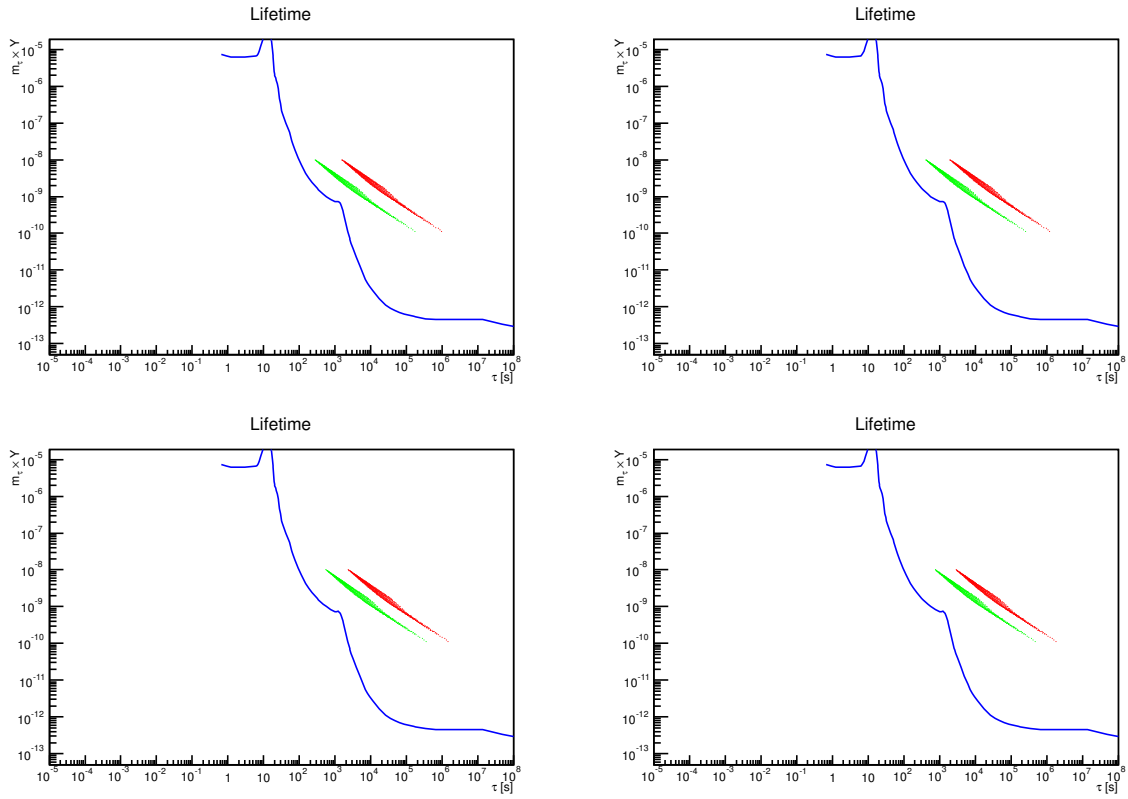

Figure 5.3.1: Graphs with yields found by micrOMEGAs against the lifetime dependent on gravitino mass found from 5.3.1. From left to right, the ratio between gaugino and gravitino given in eq. 5.3.1 determined for D=5: 0.22, 0.24, 0.26 and 0.28, and for D=6: 0.12, 0.14, 0.16 and 0.18. If any point of the D=5 set (red) and D=6 set (green) falls above or to the right of the BBN bounds (blue) they are not viable as candidates for NLSP.

5.3.2 Stau yields for D=6

Considering the same region of compactification M_c, as in Chapter 5.3.1, for D=6 the region the values of $\left(\frac{m_{3/2}}{m_{1/2}}\right)_{min}$ corresponds to a range from 0.12 to 0.18. The yields, marked with green in Fig.5.3.1 to Fig.5.3.6, still fall in the disallowed region for all three approximations when not considering late time entropy production. The results when taking the entropy production into account does push the region of high yields and short lifetimes into the allowed region, as seen in Fig.5.3.4. For the region of 0.12 and 0.14, a notable third of the points fall in the allowed region below the BBN constraints.

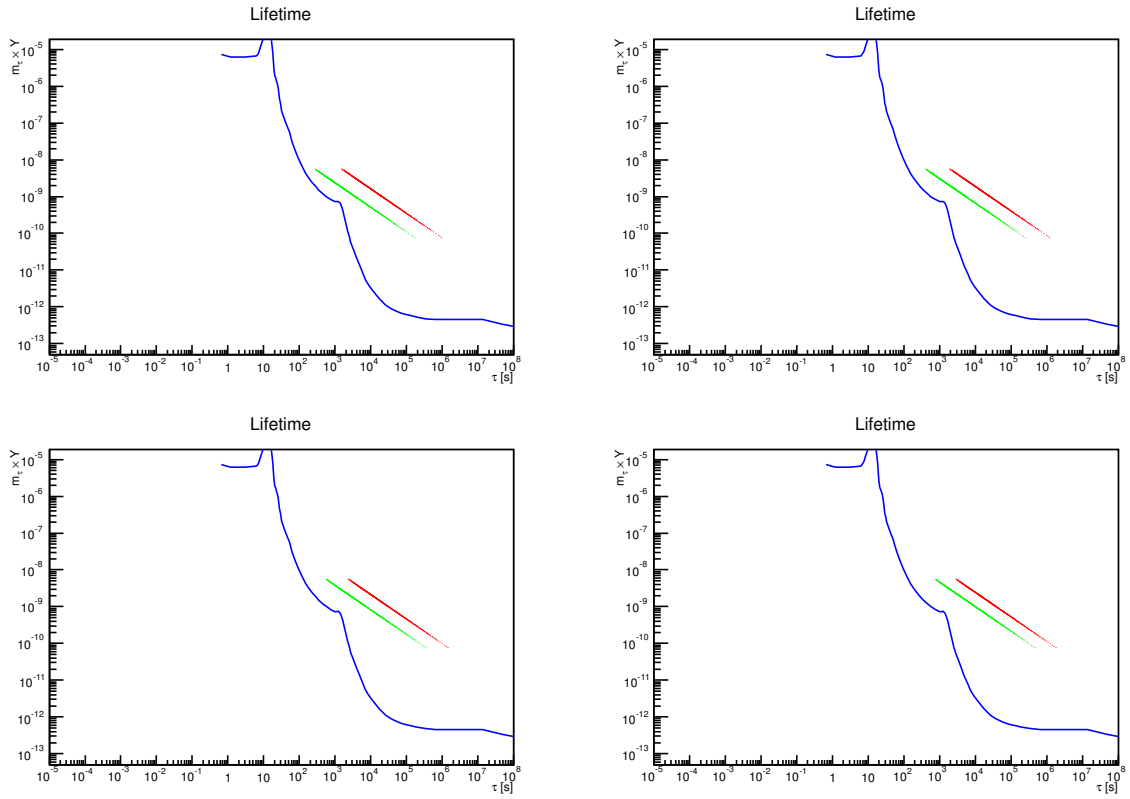

Figure 5.3.2: Graphs with yields found by eq.5.2.1 against the lifetime dependent on gravitino mass found from 5.3.1. From left to right, the ratio between gaugino and gravitino given in eq.5.3.1 determined for D=5: 0.22, 0.24, 0.26 and 0.28, and for D=6: 0.12, 0.14, 0.16 and 0.18. If any point of the D=5 set (red) and D=6 set (green) falls above or to the right of the BBN bounds (blue) they are not viable as candidates for NLSP.

5.4 Discussion

Consider the lifetime dependent on gaugino mass found using eq. 5.3.1 compared to the lifetime found with eq. 4.4.1. We can clearly see that the case of lifetime dependent on the gaugino mass, does not fit well for the region of $M_c \approx 1 \sim 2 \times 10^{16}$ and $D = 5$, as the abundances from micrOMEGAs do not fall in the allowed region. This case marked with red in Fig.5.3.4 to Fig.5.3.6. Even for the case of $m_{3/2} \sim 0.12$ to $m_{3/2} \sim 0.18 m_{1/2}$, for $M_c \approx 1 \sim 2 \times 10^{16}$ and $D = 6$, only a handful points with short lifetimes and high abundance cases become allowed, marked with green in Fig.5.3.4 to Fig.5.3.6. Adjusting the Value of

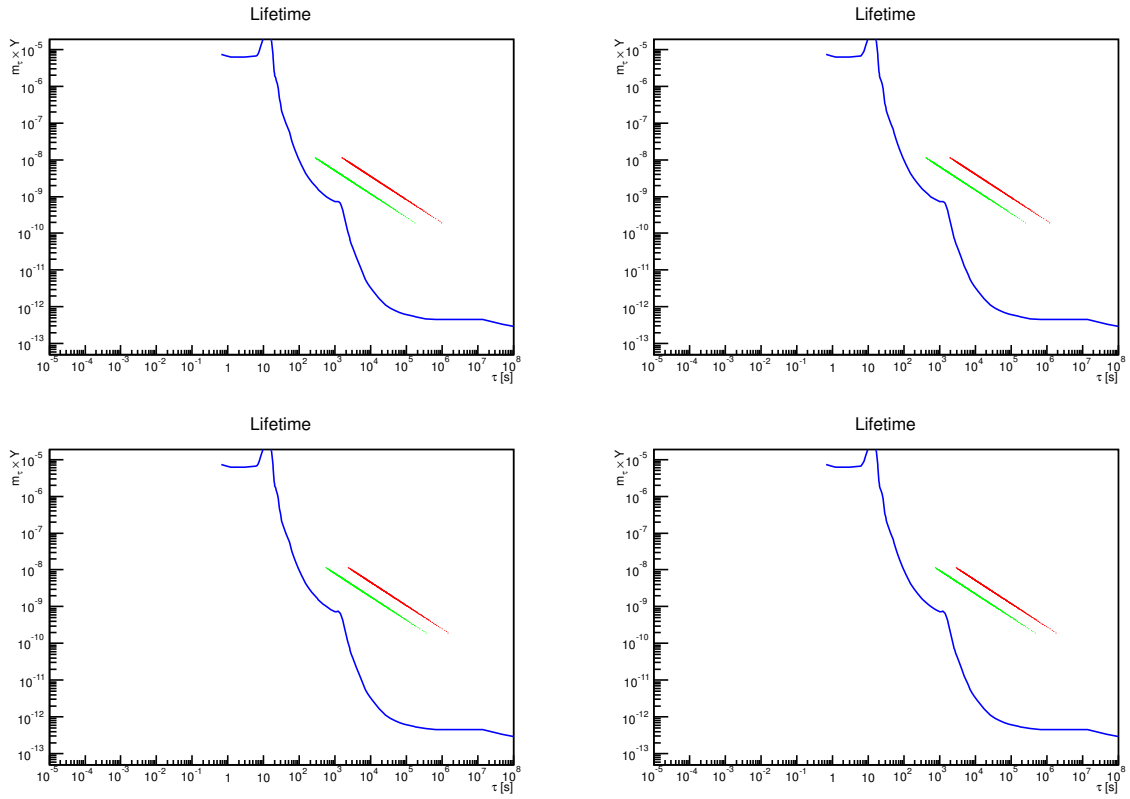

Figure 5.3.3: Graphs with yields found by using eqs.5.2.2 against the lifetime for dynamic gravitino mass found from 5.3.1.From left to right, the ratio between gaugino and gravitino given in eq. 5.3.1 determined for D=5: 0.22, 0.24, 0.26 and 0.28, and for D=6: 0.12, 0.14, 0.16 and 0.18. If any point of the D=5 set (red) and D=6 set (green) falls above or to the right of the BBN bounds (blue) they are not viable as candidates for NLSP.

M_c for $D = 5$ yields no significant change in the number of points found in the allowed region until values of $M_c \sim 10^7$GeV.

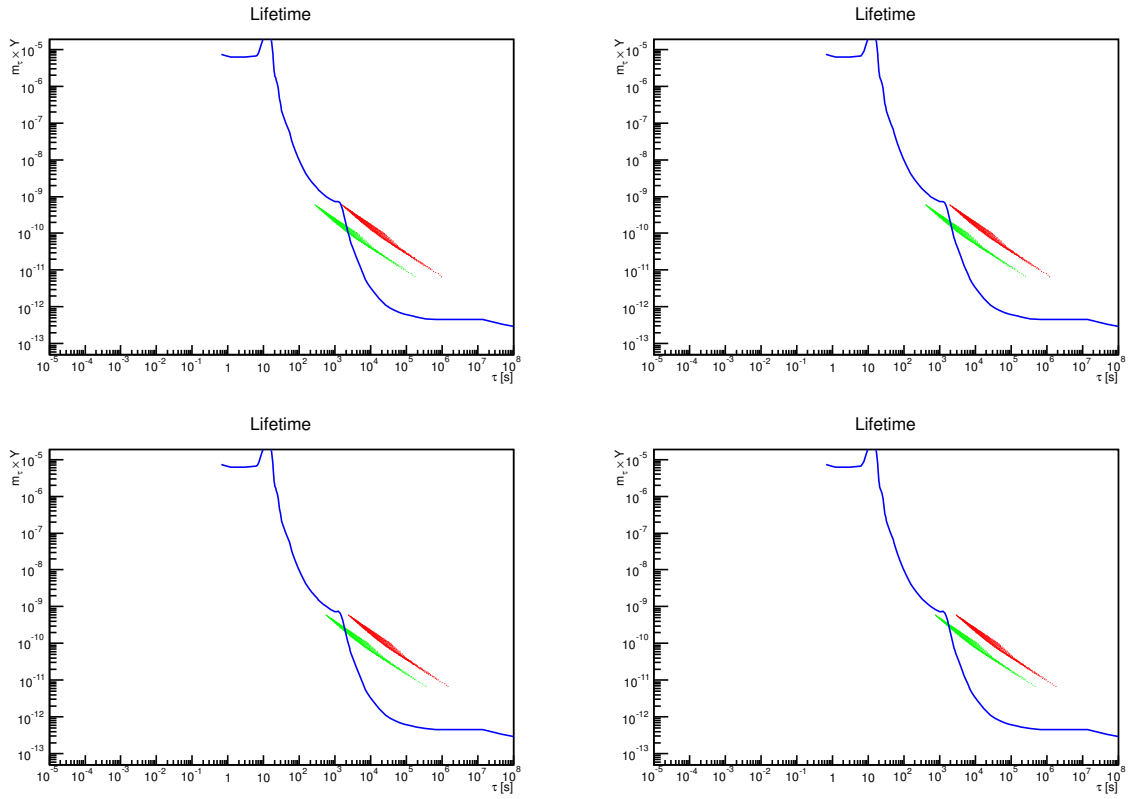

Figure 5.3.4: Graphs with yields found by using micrOMEGAs against the lifetime dependent on gravitino mass found from 5.3.1 and for $\Delta = 2 \times 10^5$ to account for late-time entropy production. From left to right, the ratio between gaugino and gravitino given in eq. 5.3.1 determined for D=5: 0.22, 0.24, 0.26 and 0.28, and for D=6: 0.12, 0.14, 0.16 and 0.18. D=5 (red), D=6 (green) and BBN bounds (blue).

For $M_c \sim 10^7$GeV for $D = 6$, the ratio between $\left(\frac{m_{3/2}}{m_{1/2}}\right)_{min}$ reaches the value of 0.05, and assuming that the points are adjusted towards the left by the reduction in this ratio, pushes wast majority, roughly 2/3 below the BBN bound. For the fixed gravitino masses, marked with red in Fig.5.1.1 to Fig.5.2.2, the generated abundances fall well within the allowed region for gravitino masses of 0.1GeV and 1GeV, both with and without taking entropy production into account.

For the case of the gravitino mass between 10GeV to 100Gev, the abundances with longer lifetimes fall within the disallowed region. A significant amount of

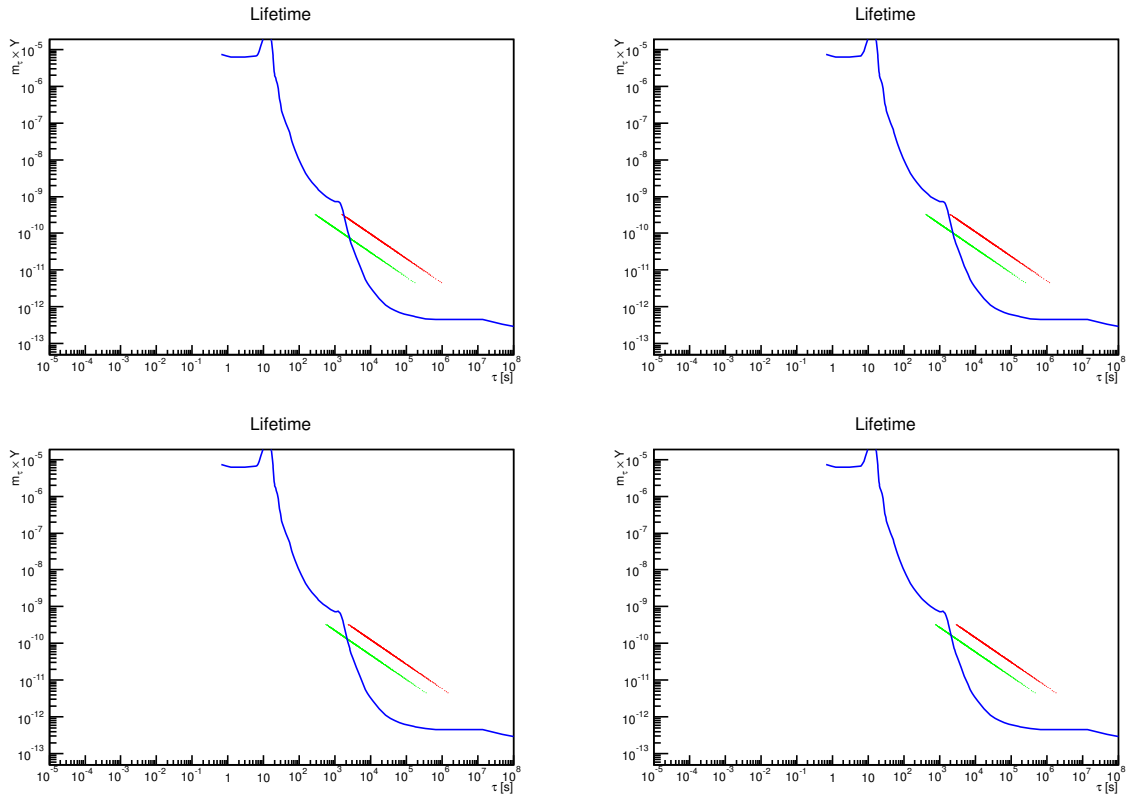

Figure 5.3.5: Graphs with yields found by eq.5.2.1 against the lifetime dependent on gravitino mass found from 5.3.1 and for $\Delta = 2 \times 10^5$ to account for late-time entropy production. From left to right, the ratio between gaugino and gravitino given in eq. 5.3.1 determined for D=5: 0.22, 0.24, 0.26 and 0.28, and for D=6: 0.12, 0.14, 0.16 and 0.18. D=5 (red), D=6 (green) and BBN bounds (blue).

points also fall above the BBN bound when adjusted for late time entropy production. As the region of gravitino masses from 0.1 to 10 Gev seems to yield a significant region of allowed staus, even without adjusting for entropy production, it stands to reason that one would expect a conservative value of the gravitino mass to be above 10GeV. Consequently, it also seems reasonable to assume the case of stau abundance from gravitino mass from eq.5.3.1 to yield more valuable results compared to the simplified yield from static gravitino mass.

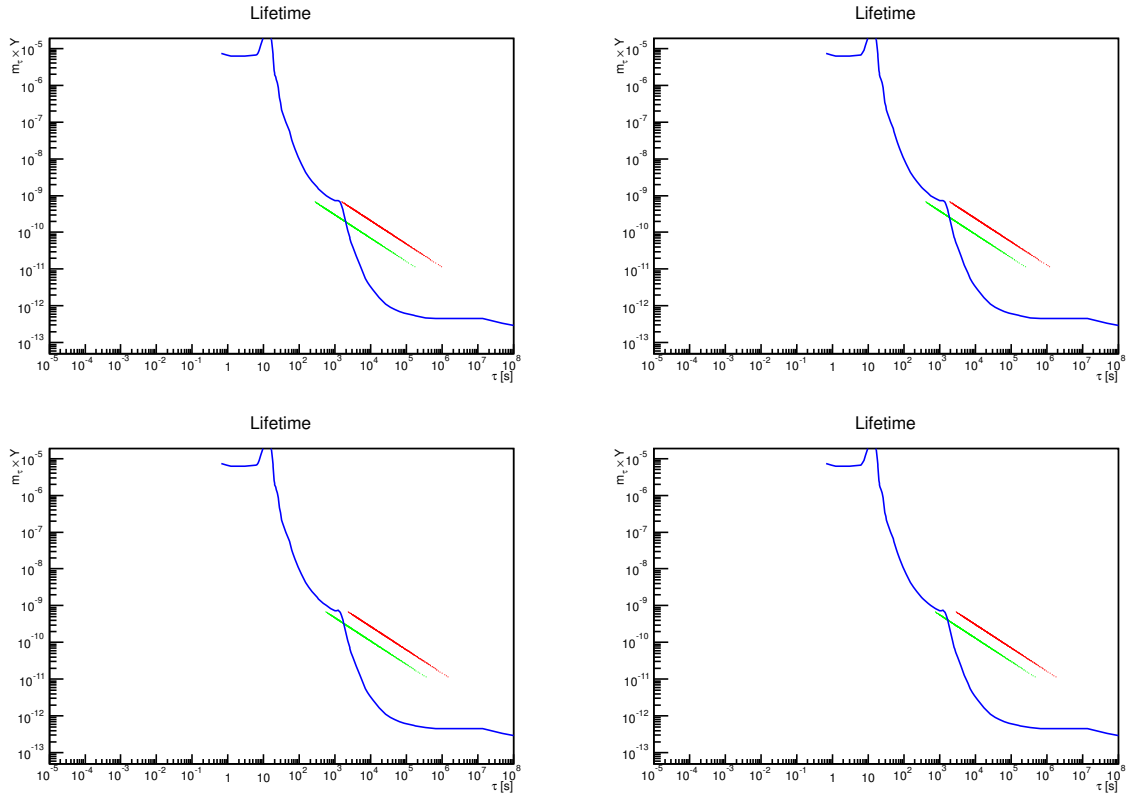

Figure 5.3.6: Graphs with yields found by eq.5.2.2 against the lifetime dependent on gravitino mass found from 5.3.1 and for $\Delta = 2 \times 10^5$ to account for late-time entropy production. From left to right, the ratio between gaugino and gravitino given in eq. 5.3.1 determined for D=5: 0.22, 0.24, 0.26 and 0.28, and for D=6: 0.12, 0.14, 0.16 and 0.18. D=5 (red), D=6 (green) and BBN bounds (blue).

Chapter 6

Open issues

In this section we will briefly discuss topics which fell outside of the scope of this thesis. Initially, in the re-expression of Leptogenesis in MSSM, it became apparent that the washout term dependent on M_1 and $\tilde{m}_1$, $\Delta W(M_1, \tilde{m}_1)$, could not be easily expressed in the same way for the sneutrino. It is likely that the interactions included in the washout would have to include terms with both the sneutrino and the neutrino masses, and as such could not be expressed in the same manner as in this thesis. In the SM scenario, the lower bound on the mass of the lightest left handed neutrino is set to zero, $m_1 = 0$ or $\beta = 1$, and since the maximal CP asymmetry, eq.3.7.1, is directly dependent on the m_1 mass, by setting it to zero the equations are greatly simplified, only dependent on M_1 for fixed m_3 mass. This correction is not large, but this m_1 contribution directly reduces the maximal CP-asymmetry, in turn reducing the maximally allowed baryon asymmetry.

Chapter 7

Conclusion

In this thesis we have considered if late time entropy production can be utilized to facilitate a stau NLSP with respect to BBN constraints. As a bound on the amount of allowed entropy production we have considered the mass of the right handed heavy neutrino and its super symmetric partner, the sneutrino, as their decays are responsible for the majority of our chosen stau NLSP. We determined the amount of produced entropy by considering the decay of a massive right handed neutrino from extended SM. This decay gave us a measure of the baryon number density, η_B, which is dependent on the mass of the lightest right handed neutrino M_1. From this dependency, we determined the peak value of M_1 with respect to η_B, and calculated the difference between the CMBR value to obtain the peak value of the entropy dilution factor. We extended the SM Leptogenesis model to MSSM by considering the additional interactions introduced, with the addition of the Sneutrino, we discovered an increase in the upper bound of entropy production by a factor of 4.

The stau abundances, generated with mircOMEGAs, match well with the abundances found by using methods in other papers [9] and [20]. The bounds of BBN limit significantly the set allowed particles with long mean lifetimes, as such it is not surprising that for the majority of points for long lifetimes can be disregarded. The region we should be interested in is then for high abundances and shorter lifetimes. The plots with gravitino mass dependent on the gaugino mass, Δ_{peak} and $D = 5$, all fall above the BNN bounds invalidating the stau as

an NLSP for $D = 5$. The same does not hold for the same case with $D = 6$, where there exists a section of points which fall below the BBN bound, yielding a region with an allowed Stau NLSP.

Chapter 8

Appendix A

8.1 Assumptions to derive η_B^{MSSM}

Under is the list of assumptions used in chapter 4.3 to find η_B^{MSSM}:

- The boltzman equation for the MSSM extension of Leptogenesis is similar for both the neutrino and the sneutrino:

$$\begin{aligned}
\frac{dN_{N_1}}{dz} &= -(D_{N_1} + S_{N_1})(N_{N_1} - {N^{eq}}_{N_1}) \\
\frac{dN_{\tilde{N}_1}}{dz} &= -(D_{\tilde{N}_1} + S_{\tilde{N}_1})(N_{\tilde{N}_1} - {N^{eq}}_{\tilde{N}_1}) \\
\frac{dN_{B-L}}{dz} &= -\tilde{\epsilon}_1^N D_{N_1}(N_{N_1} - {N^{eq}}_{N_1}) - \tilde{\epsilon}_1^{\tilde{N}} D_{\tilde{N}_1}(N_{\tilde{N}_1} - {N^{eq}}_{\tilde{N}_1}) - W N_{B-L}
\end{aligned} \tag{8.1.1}$$

  where $\tilde{\epsilon}_1^{\tilde{N}}$ and $\tilde{\epsilon}_1^N$ are CP violating terms for the sneutrino and neutrino respectively.

$$\begin{aligned}
\tilde{\epsilon}_1^{\tilde{N}} &= \tilde{\epsilon}_l^{\tilde{N}^*} + \tilde{\epsilon}_{\tilde{L}}^{\tilde{N}} \\
\tilde{\epsilon}_1^N &= \tilde{\epsilon}_l^N + \tilde{\epsilon}_{\tilde{L}^*}^N
\end{aligned} \tag{8.1.2}$$

- The efficiency factor κ can be found by evaluating the integral derived from the boltzmann equations in eq.8.1.1 [11, 15].

$$\begin{aligned}
\kappa(z) = &-\frac{4}{3}\int_{z_i}^{z} dz' \frac{D_{N_1}}{D_{N_1} + S_{N_1}} \frac{dN_{N_1}}{dz'} e^{-\int_{z'}^{z} dz'' W_{N_1}(z'')} \\
&-\frac{4}{3}\int_{z_i}^{z} dz' \frac{D_{\tilde{N}_1}}{D_{\tilde{N}_1} + S_{\tilde{N}_1}} \frac{dN_{\tilde{N}_1}}{dz'} e^{-\int_{z'}^{z} dz'' W_{\tilde{N}_1}(z'')} + F(m_{N_1}, m_{\tilde{N}_1})
\end{aligned} \tag{8.1.3}$$

where $F(m_{N_1}, m_{\tilde{N}_1})$ is the interference terms for the washout interactions between the neutrino and the snautrino, and assumed to be negligible compared to the size of the two integrals. Since the decay width and scattering terms can be assumed to separately be of the same order, we can once again can assume that these integrals also can be taken to be of the same order, and so we gain a factor of 2.

$$\kappa^{MSSM} = 2\kappa^{SM} \tag{8.1.4}$$

Valid when the $\Delta L = 2$ corrections are neglected.

- For the CP asymmetry generated by the new processes introduced from extension into MSSM, we can find[14]:

$$\tilde{\epsilon}_i = \tilde{\epsilon}_l^{N_i} + \tilde{\epsilon}_{\tilde{L}^*}^{N_i} + \tilde{\epsilon}_l^{\tilde{N}_i^*} + \tilde{\epsilon}_{\tilde{L}}^{\tilde{N}_i} = 4\tilde{\epsilon}_l^{N_i} \tag{8.1.5}$$

Where $\tilde{\epsilon}_l^{N_i}$ is the MSSM CP asymmetry generated from the decay of the neutrino into a lepton-higgs final state. The contribution to the asymmetry from this decay can be separated into two different style of diagrams, radiative corrections and vertex corrections, represented in fig. 4.3.1a and fig. 4.3.1b respectively.

$$\tilde{\epsilon}_l^{N_i} = \tilde{\epsilon}_l^{N_i}(wave) + \tilde{\epsilon}_l^{N_i}(vertex) \tag{8.1.6}$$

The diagrams which contribute to radiative and vertex corrections are doubled when going from SM to the MSSM, and by directly calculating the set of asymmetries from eq. 4.3.4 we find contributions of the form[14]:

$$\begin{aligned} \tilde{\epsilon}_l^{N_i}(vertex) &= -\frac{1}{8\pi}\sum_k g(y_k)\mathcal{I}_{ki} \\ \tilde{\epsilon}_l^{N_i}(wave) = 2\epsilon_l^{N_i}(wave) &= -\frac{1}{4\pi}\sum_{k\neq i}\frac{M_i M_k}{M_k^2 - M_i^2}\mathcal{I}_{ki} \end{aligned} \tag{8.1.7}$$

Where is defined as $g(x) = \ln\frac{(1+x)}{x}$. Now considering the other decay channels for the neutrino and sneutrino the result is the contribution is equal vertex and wave correction, are all of similar size.

$$\begin{aligned} \tilde{\epsilon}_l^{N_i}(wave) = \tilde{\epsilon}_{\tilde{L}^*}^{N_i}(wave) = \tilde{\epsilon}_l^{\tilde{N}_i^*}(wave) = \tilde{\epsilon}_{\tilde{L}}^{\tilde{N}_i}(wave) \\ \tilde{\epsilon}_l^{N_i}(vertex) = \tilde{\epsilon}_{\tilde{L}^*}^{N_i}(vertex) = \tilde{\epsilon}_l^{\tilde{N}_i^*}(vertex) = \tilde{\epsilon}_{\tilde{L}}^{\tilde{N}_i}(vertex) \end{aligned} \tag{8.1.8}$$

The CP asymmetry contriubtion from each of these corrections present in MSSM is therefore twice the size, and one finds the relation $\tilde{\epsilon}_l^{N_i} = 2\epsilon_i^{N_i}$. As such we gain a total factor of 8 when considering the 3 additional interactions which generate CP-asymmetry in the MSSM scenario.

- We need the strength of the total washout to be of the order similar to the SM washout, $\mathcal{O}(W^{SM}) \simeq \mathcal{O}(W^{MSSM})$. Additionally, the washout processes related to $\Delta L = 2$ interactions have need to have negligible interference terms between the neutrino and sneutrino, $\Delta W = \Delta W(M_{N_1}) + \Delta W(M_{\tilde{N}_1})$.

- We require the low temperature limit of $\Delta W(M_{\tilde{N}_1})$ is similar to the neutrino limit found in eq. 3.6.2.

Bibliography

[1] F. Mandl, G. Shaw, "Quantum Field Theory" 2010 ISBN 978-0-471-49684-7

[2] C. Burgess, G. Moore, 2006. "The standard model: A primer". ISBN 9780511254857

[3] S.P. Martin, 2011 "A supersymmetry primer" *Adv. Ser. Direct. High Energy Phys*, 21(515), pp.1-153 arXiv preprint hep-ph/9709356

[4] M. Lindner, T.Ohlsson, G. Seidl, 2002 "Seesaw mechanisms for Dirac and Majorana neutrino masses" *Physical Review D*, 65(5), p.053014. arXiv:hep-ph/0109264

[5] H. Baer (Florida State U.) , X. Tata (Hawaii U.) "Weak Scale Supersymmetry: From Superfields to Scattering Events" Cambridge University Press (2006-05-31) ISBN: 0521290317, 9780521290319,

[6] W. Buchmüller, P. Di Bari, M. Plümacher, 2004. "Some aspects of thermal Leptogenesis" *New Journal of Physics*, 6(1), p.105. arXiv:hep-ph/0406014v1

[7] E. W. Kolb, M. S. Turner "The Early Universe" 1990 ISBN 0-201-11603-0

[8] J. Hasenkamp, J. Kersten, 2010. "Leptogenesis, gravitino dark matter, and entropy production" *Physical Review D*, 82(11), p.115029. arXiv:1008.1740 [hep-ph]

[9] M. Kawasaki, K. Kohri, T. Moroi, A. Yotsuyanagi, 2008. "Big-bang nucleosynthesis and gravitinos" *Physical Review D*, 78(6), p.065011. arXiv:0804.3745 [hep-ph]

[10] M. Pospelov, 2007. "Particle physics catalysis of thermal big bang nucleosynthesis" *Physical review letters*, 98(23), p.231301. arXiv:hep-ph/0605215

[11] W. Buchmüller, P. Di Bari, M. Plümacher, 2005. "Leptogenesis for pedestrians" *Annals of Physics*, 315(2), pp.305-351. arXiv:hep-ph/0401240v1

[12] W. Buchmüller, P. Di Bari, M. Plümacher, 2003. "The neutrino mass window for baryogenesis"*Nuclear Physics B*, 665, pp.445-468. arXiv:hep-ph/0302092

[13] W. Buchmüller, M. Plümacher, 1998. "CP asymmetry in Majorana neutrino decays" *Physics Letters B*, 431(3), pp.354-362. arXiv:hep-ph/9710460

[14] L.Covi, E.Roulet, F.Vissani, 1996. "CP violating decays in Leptogenesis scenarios" *Physics Letters B*, 384(1), pp.169-174. arXiv:hep-ph/9605319v2

[15] W. Buchmüller, P. Di Bari, M. Plümacher, 2002. "Cosmic microwave background, matter-antimatter asymmetry and neutrino masses" *Nuclear Physics B*, 643(1), pp.367-390. arXiv:hep-ph/0205349v2

[16] G.F. Giudice, A. Notari, M. Raidal, A. Riotto, A. Strumia, 2004. "Towards a complete theory of thermal Leptogenesis in the SM and MSSM" *Nuclear Physics B*, 685(1), pp.89-149. arXiv:hep-ph/0310123

[17] G. Belanger, F. Boudjema, A. Pukhov, A. Semenov, 2014. "micrOMEGAs_3: A program for calculating dark matter observables." *Computer Physics Communications*, 185(3), pp.960-985. arXiv:1305.0237 [hep-ph]

[18] W. Buchmüller, K. Hamaguchi, M. Ratz, T.Yanagida, 2004. "Supergravity at colliders" *Physics Letters B*, 588(1), pp.90-98. arXiv:hep-ph/0402179

[19] G. Belanger, F. Boudjema, S. Kraml, A. Pukhov, A. Semenov , 2006. "Relic density of neutralino dark matter in the MSSM with C P violation" *Physical Review D*, 73(11), p.115007. arXiv:hep-ph/0604150

[20] J.Heisig, J. Kersten, B. Panes, T. Robens 2013. A survey for low stau yields in the MSSM. arXiv preprint arXiv:1310.2825. arXiv:1310.2825 [hep-ph]

[21] W. Buchmüeller, K. Hamaguchi, J. Kersten, 2006. "The gravitino in gaugino mediation" *Physics Letters B*, 632(2), pp.366-370. arXiv:hep-ph/0506105

Acknowledgements

It is a pleasure to thank my advisor jörn Kersten and my friend and fellow student Håkon Høines for interesting discussions on diverse topics throughout the writing of this thesis. I would also like to thank my colleagues Andreas, Hans, Are, Magne, Simen, Inga and Nick for their motivation and comradery. Finally I would like to thank my family and friends for their continued support.